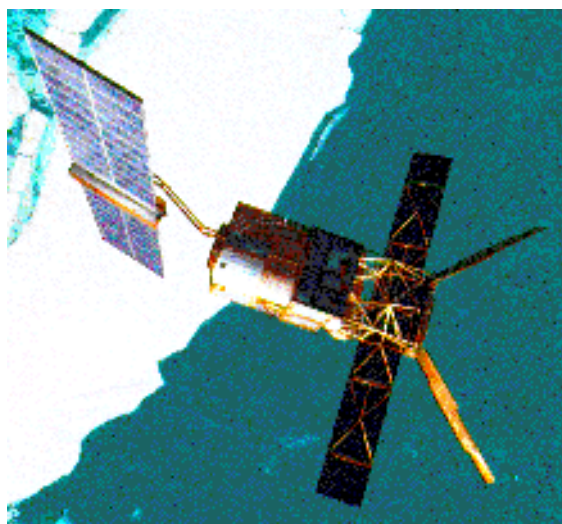


# ERS-2 Wind Scatterometer Cyclic Report

from 8<sup>th</sup> March 2004 to 12<sup>th</sup> April 2004  
Cycle 93



---

Prepared by:

PCS team

ESRIN EOP-GOQ

Inputs from:

F. Aidt  
H. Hersbach

ESTEC TOS-EMS  
ECMWF

Issue: 1.0  
Reference: ERSE-SPPA-EOPG-TN-04-0004  
Date of issue: 14<sup>th</sup> June 2004  
Status: Approved  
Document type: Technical Note  
Approved by: P. Lecomte

A handwritten signature in black ink, appearing to read 'Lecomte', written over a white background.

# Distribution List

(Summary only via e-mail)

ESTEC	M. Canela	EOP-PEL
	E. Attema	EOP-SMS
	M. Drinkwater	EOP-SMO
	F. Aidt	TOS-EMS
	B. Gelsthorpe	EOP-PTR
	R. Zobl	EOP-P
	K. van't Klooster	TOS-EEA
ESOC	F. Bosquillon de Frescheville	TOS-OFE
	L. Stefanov	TOS-OF
ESRIN	M. Albani	EOP-GO
	P. Lecomte	EOP-GOQ
	V. Beruti	EOP-GOF
	S. Jutz	EOP-GOU
	W. Lengert	EOP-GM
	G. Kohlhammer	EOP-G
	M. Onnestam	EOP-GOC
	G. Emiliani	EOP-GOQ-PCS
L.A. Breivik		DNMI
P. Snoeij		DUT
J. Heidebreder		DORNIER
L. Isaksen, H. Hersbach		ECMWF
J. Kerkman, J. Figa		EUMETSAT
V. Wismann		IFARS
R. Ezraty		IFREMER
R.S. Dunbar		JPL
A. Stoffelen, T. Driessenaar		KNMI
G. Legg, P. Chang		NOAA/NESDIS
W. Gemmill		NOAA/NWS
J. Hawkins		NRL
D. Offiler, R. Graham, C.A. Parrette		UK-MET Office
F. Courtier, H. Roquet		Meteo-France
C. Scupniewicz		FNMOG
R.A. Brown		University of Washington
J. Boutin		LODYC/UPMC
M.A. Messeh		University of Sheffield

This report is available on PCS web:  
[http://earth.esa.int/pcs/ers/scatt/reports/pcs\\_cyclic/](http://earth.esa.int/pcs/ers/scatt/reports/pcs_cyclic/)

## **1.0 Introduction and summary**

The document includes a summary of the daily quality control made within the PCS and various sections describing the results of the investigations and studies of “open-problems” related to the Scatterometer. In each section results are shown from the beginning of the mission in order to see the evolution and to outline possible “seasonal” effects. An explanation for the major events which have impacted the performance since launch is given, and comments about the recent events which occurred during the last cycle are included.

This report covers the period from 8<sup>th</sup> March 2004 to 12<sup>th</sup> April 2004 to (cycle 93) and includes the results of the monitoring activity performed by ESRIN and ECMWF.

### **Mission events**

- The ERS-2 satellite was piloted in ZGM throughout the cycle 93.
- During cycle 93 the ESACA processor worked nominally without faults.
- The AMI instrument was unavailable on 8 April 2004 from 6 a.m. to 10 a.m.
- Since March, 3<sup>rd</sup> Matera (South Italy) ground station is acquiring low rate bit data for all the passes for which is planned a SAR acquisition. Some science data are produced and disseminated to the users, Radar Altimeter data, Wave data and Scatterometer data are recorded on tapes and will be available off-line for re-processing. This means for the Scatterometer data coverage a very limited improvement due to the fact that are acquired only the passes for which some SAR activity is planned.
- For the entire period in cycle 93, ERS-2 scatterometer data was used in the 4D-Var data assimilation system at ECMWF. The re-introduction of the UWI data occurred just prior to the start of cycle 93, and makes now use of CMOD5-based winds. Since cycle 59 in January 2001, this is the first 5-weekly period for which UWI data was assimilated at ECMWF.

### **Yaw performance**

- The result of the yaw monitoring for cycle 93 is a yaw error angle within the expected nominal range (+/- 2 degrees) with an average level around 0 deg. for most of the orbit. On 23 and 28 March 2004 some orbits had a bad quality yaw performances due to the satellite manoeuvres occurred on those days. At the node level, the combined kp and yaw-error flag was set, allowing the users to reject the low quality measurements.

### **Calibration performance**

- Calibration data from Transponder are regularly acquired and archived for re-processing. The CALPROC processor is not able to produce accurate gain constant with the actual degraded satellite attitude. For that reason ESRIN had initiated the TOSCA (Tool for Scatterometer Calibration) project to re-design the calibration processor and re-compute valid gain constants coefficients.
- Due to the regional mission scenario the calibration performances over the Brazilian rain forest are not available because that area is not covered by the ESA ground station. The chance to install a new station to cover the calibration site is under investigation as well as the possibility to use stable ice area in Greenland to monitor the instrument calibration.

- The Ocean Calibration monitoring is performed by ECMWF. Compared to cycle 92, bias levels have become around 0.4 more negative for descending tracks and 0.3 dB for ascending tracks in a rather uniform way. The situation is similar to that for nominal data in 2000, although the inter-node trends were larger. For cycle 93 such variations over incidence angle are small. Bias levels are in between -0.2 and -0.7 dB.

### Instrument performance

- During the cycle 93 the mean transmitted power decrease has been 0.04dB per cycle. That value confirms the tendency noted for the cycle 92 towards a stabilization of the transmitted power evolution.
- The evolution of the noise during the cycle 93 was stable. The daily average noise power for the Fore and Aft beam was around 1.7 ADC (I) and around 1.6 ADC (Q) respectively. For the Mid beam the noise is not measurable.
- During the cycle 93 the Doppler compensation evolution was very stable. The averaged CoG of the compensated spectrum is very close to zero for the Fore and Aft beam and around 200Hz for the Mid beam. The CoG standard deviation was around 1600 Hz for the Fore and Aft antenna and around 2700 Hz for the Mid antenna. The small peak detected on 23rd March 2004 was due to an AOCS mode-change to FPM in order to perform an orbit manoeuvre.

### Product performance

- During cycle 93, data was received between 21:06 UTC 8 March 2004 and 20:59 UTC 12 April 2004. Data was received for all 6-hourly batches, however, for 06 UTC 24 March 2004 (due to dissemination problem) and 06 UTC 08 April 2004 very low amounts were recorded (due to an AMI anomaly occurred on that day).
- Compared to cycle 92, the agreement with ECMWF first-guess (FGAT) fields has improved with regard to relative standard deviation (from 1.67 m/s to 1.54 m/s). However, the relative bias has become larger (from -0.51 m/s to -0.70 m/s). A small part of the reduced random deviations is expected to result from the re-introduction of UWI data in the assimilation system. However, the impact on the monitor statistics would have been larger if ECMWF analysis winds would have been used, rather than FGAT. Another, probably larger part of the reduction, must originate from the seasonal trend of the regional data set, which makes an objective judgment on the quality of the UWI product difficult. The larger negative bias of the UWI winds seems more objective. This conjecture is confirmed by a similar trend in the backscatter levels. Both standard deviations and bias levels of wind speed are better to those for 2000. The quality of both UWI and de-aliased CMOD4 wind direction has improved. As stated above, the ECMWF assimilation system was not changed during cycle 93, though just before the start of this period (for details see report for cycle 92)
- The PCS geophysical monitoring reports a wind speed bias (18 or 24 hour forecast vs UWI) around 0.5 m/s and a wind speed standard deviation around 1.5 m/s. The wind direction deviation has improved. Roughly the 98% (it was 96% for cycle 92) of the nodes have a wind direction in agreement with the meteorological forecast.

## **2.0 Calibration Performances**

The calibration performances are estimated using three types of target: a man made target (the transponder) and two natural targets (the rain forest and the ocean). This approach allow us to design the correct calibration using a punctual but accurate information from transponders and an extended but noisy information from rain forest and ocean for which the main component of the variance comes from the geophysical evolution of the natural target and from the backscattering models used. These aspects are in the calibration performance monitoring philosophy. The major goals of the calibration monitoring activities are the achievement of a “flat” antenna pattern profile and the assurance of a stable absolute calibration level.

### **2.1 Gain Constant over transponder**

One gain constant is computed per transponder per beam from the actual and simulated two-dimensional echo power, which is given as a function of the orbit time and range time. This parameter clearly indicates the difference between “real instrument” and the mathematic model. In order to acquire data over the transponder the Scatterometer must be set in an appropriate operational mode defined as “Calibration Mode”.

Since January 2001 with the operations in Zero Gyro Mode (ZGM) the satellite attitude is not stable as it was in the nominal Yaw Steering Mode (YSM). In particular there is a non-predictable variation of the yaw error angle along the orbit. For that reason the gain constant data computed by the CALPROC processor, that assumes a stable orbit, are meaningless and a new calibration processor is under development. In the mean time, data from the Transponder are still acquired and archived for future re-processing. The reprocessed gain constants will be provided in this section when available.

For the gain constant computed during the nominal YSM please refer to the Scatterometer cyclic report - cycle 60 -

### **2.2 Ocean Calibration**

The Scatterometer sigma noughts were compared with the ECMWF model first guess winds. The result is shown in Figure 1 as the ratio of  $\langle \sigma_0^{0.625} \rangle / \langle \text{CMOD4(First Guess)}^{0.625} \rangle$  converted in dB for the for beam (solid line), mid beam (dashed line) and aft beam (dotted line), as a function of incidence angle for descending and ascending tracks. The thin lines indicate the error bars on the estimated mean. First-guess winds are based on the in time closest (+3h, +6h, +9h, or +12h) T511 forecast field, and are bilinearly interpolated in space.

Compared to cycle 92, bias levels have become around 0.4 more negative for descending tracks and 0.3 dB for ascending tracks in a rather uniform way. The situation is similar to that for nominal data in 2000, although then inter-node trends were larger. For cycle 93 such variations over incidence angle are small. Bias levels are in between -0.2 and -0.7 dB.

The data volume of ascending and descending tracks are nearly equal.

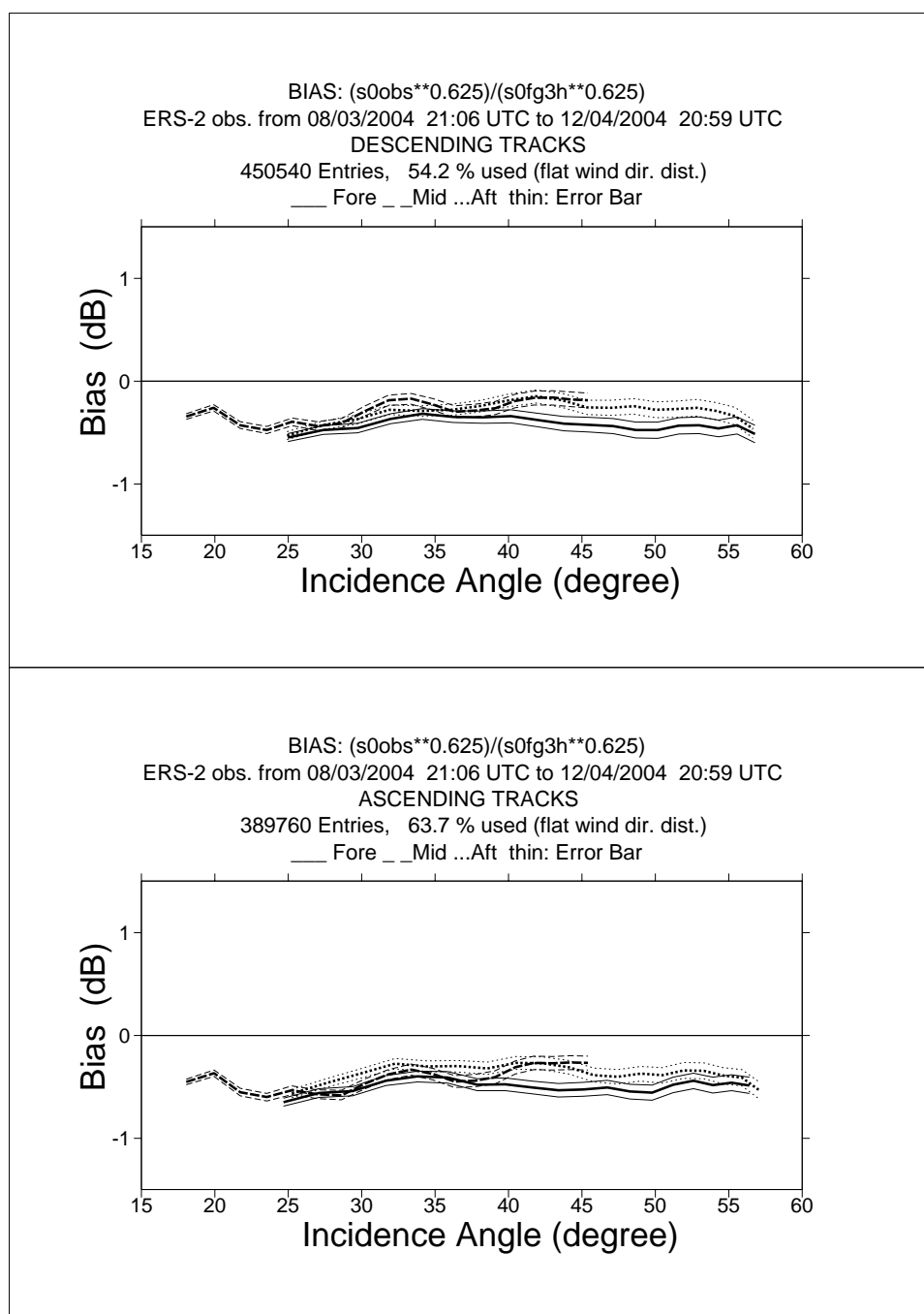


**FIGURE 1.** ERS-2 Scatterometer Ocean Calibration cycle 93. Ratio of  $\langle \sigma_0^{0.625} \rangle / \langle \text{CMOD4}(\text{First Guess})^{0.625} \rangle$  converted in dB for the fore beam (solid line), mid beam (dashed line) and aft beam (dotted line), as a function of incidence angle for descending and ascending tracks. The thin lines indicate the error bars on the estimated mean. First-guess winds are based on the in time closest (+3h, +6h, +9h, or +12h) T511 forecast field, and are bilinearly interpolated in space.

## 2.3 Gamma-nought over Brazilian rain forest

Although the transponders give accurate measurements of the antenna attenuation at particular points of the antenna pattern, they are not adequate for fine tuning across all incidence angles, as there are simply not enough samples. The tropical rain forest in South America has been used as a reference distributed target. The target at the working frequency (C-band) of ERS-2 Scatterometer acts as a very rough surface, and the transmitted signal is equally scattered in all directions (the target is assumed to follow the isotropic approximation). Consequently, for the angle of incidence used by ERS-2 Scatterometer, the normalised backscattering coefficient (sigma nought) will depend solely on the surface effectively seen by the instrument:

$$S^0 = S \cdot \cos \theta$$

With this hypothesis it is possible to define the following formula:

$$\gamma^0 = \frac{\sigma^0}{\cos \theta}$$

Using this relation, the gamma nought backscattering coefficient over the rain forest is independent of the incident angle, allowing the measurements from each of the three beams to be compared.

The test area used by the PCS is located between 2.5 degrees North and 5.0 degrees South in latitude and 60.5 degrees West and 70.0 degrees West in longitude. That area is actually not covered by the Regional mission scenario (since cycle 86 onwards) and therefore the calibration monitoring activity over the Brazilian rain forest is suspended because no data are available.

The chance to continue the monitoring activity with a new receiving station covering the Brazilian rain forest is under investigation. The following paragraphs will report on the results when data will be available.

### 2.3.1 Antenna pattern: Gamma-nought as a function of elevation angle

Due to the regional mission scenario data over the Brazilian rain forest are not available. For that reason the antenna patterns in function of the elevation angle have not been computed.

### 2.3.2 Antenna pattern: Gamma-nought as a function of incidence angle

Due to the regional mission scenario data over the Brazilian rain forest are not available. For that reason the antenna patterns in function of the incidence angle have not been computed



### 2.3.3 Gamma nought histograms and peak position evolution

As the gamma nought is independent from the incidence angle, the histogram of gamma noughts over the rain forest is characterised by a sharp peak. The time-series of the peak position gives some information on the stability of the calibration. This parameter is computed by fitting the histogram with a normal distribution added to a second order polynomial:

$$F\langle x \rangle = A_0 \cdot \exp\left(-\frac{z^2}{2}\right) + A_3 + A_4 \cdot x + A_5 \cdot x^2$$

where:  $z = \frac{x - A_1}{A_2}$

The parameters are computed using a non linear least square method called “gradient expansion”. The position of the peak is given by the maximum of the function  $F(x)$ . The histograms are computed weekly (from Monday to Sunday) for each antenna individually (“Fore”, “Mid”, and “Aft”) and for ascending and descending passes with a bin size of 0.02 dB.

Due to the regional mission scenario data over the Brazilian rain forest are not available and the, the histograms have not been computed.

For the time series since the beginning of the mission please refer to the Scatterometer cyclic report cycle 86.

### 2.3.4 Gamma nought image of the reference area

Due to the regional mission scenario data over the Brazilian rain forest are not available and the, the histograms have not been computed

### 2.3.5 Sigma nought evolution

Due to the regional mission scenario data over the Brazilian rain forest are not available. For that reason no update has been done to the sigma nought evolution time series.

For the time series since the beginning of the mission until June 2003 please refer to the Scatterometer cyclic report cycle 86.

### 2.3.6 Antenna temperature evolution over the Rain Forest

Due to the regional mission scenario data over the Brazilian rain forest are not available.

For the time series since the beginning of the mission please refer to the Scatterometer cyclic report cycle 86.



### **3.0 Instrument performance**

The instrument status is checked by monitoring the following parameters:

- Centre of Gravity (CoG) and standard deviation of the received signal spectrum. This parameter is useful for the monitoring of the orbit stability, the performances of the doppler compensation filter, the behaviour of the yaw steering mode and the performances of the devices in charge for the satellite attitude (e.g. gyroscopes, Earth sensor, Sun sensor).
- Noise power I and Q channel.
- Internal calibration pulse power.

the latter is an important parameter to monitor the transmitter and receiver chain, the evolution of pulse generator, the High Power Amplifier (HPA), the Travelling Wave Tube (TWT) and the receiver.

These parameters are extracted daily from the UWI products and averaged. The evolution of each parameter is characterised by a least square line fit. The coefficients of the line fit are printed in each plot.

#### **3.1 Centre of gravity and standard deviation of received power spectrum**

The Figure 2 shows the evolution of the two parameters for each beam for the long term monitor and Figure 3 shows the same for the cycle 93.

The tendency from the beginning of the mission to the operation with the new Mono Gyro (MGM) Attitude On-board Control System (AOCS) configuration (7<sup>th</sup> February 2000) is a clear and regular small increase of the Centre of gravity (CoG) of received spectrum for the three antennae. An increase of roughly 200 Hz was observed at the end of the MGM qualification period. After the AOCS commissioning phase this parameter further evolved.

The nominal 3-gyroes AOCS configuration (plus one Digital Earth Sensor - DES, and one Digital Sun Sensor - DSS and backups) was no more considered safe because 3 of the six gyros on-board were out of order or very noisy. The MGM configuration was designed to pilot the ERS-2 using only one gyro plus the DES and the DSS modules. Scope of ZGM configuration was to extend the satellite lifetime by using the available gyros one at the time.

With MGM configuration, the gyro 5 was used until 7<sup>th</sup> October 2000 when it failed. From 10<sup>th</sup> October 2000 to 24<sup>th</sup> October 2000 the gyro 6 was used. This explains the decrease of roughly 100Hz in the CoG of the received spectrum. From 25<sup>th</sup> October 2000 to 17<sup>th</sup> January 2001 the gyro 1 was used to pilot the ERS-2 satellite.

On 17<sup>th</sup> January 2001 the AOCS was upgraded. The new configuration allows to pilot the satellite without gyroscopes. Unfortunately a failure of the Digital Earth Sensor (DES A-side) caused ERS-2 to enter in Safe-Mode on the same day. On 25<sup>th</sup> January 2001 gyro #1 also failed. During the period of safe mode the spacecraft had drifted out of the nominal deadband by some 30 Km. The nominal orbit was reached on 6<sup>th</sup> February 2001.

In order to preserve the remaining gyroscope for further manoeuvres, ERS-2 will now being operated in Extra Backup Mode (EBM). The EBM is a coarse attitude control mode. An upgrade of

EBM has been performed on 30<sup>th</sup> March 2001. The aim of the upgrade was to introduce the Yaw steering law inside the piloting function. The new configuration has been renamed as EBM-YSM.

Since 7<sup>th</sup> June 2001 a new AOCS configuration is active on board. The purpose of the Zero Gyro Mode (ZGM) is to improve the yaw performances without use of gyroscope.

Until 17<sup>th</sup> January 2001 the evolution of the standard deviation of the CoG of the received spectrum was stable apart from the change occurred on 26<sup>th</sup>, October 1998. On October 26<sup>th</sup>, 1998 the standard deviation of the CoG had, on average, a decrease of roughly 100 Hz for the fore and aft antenna and of roughly 30Hz for the mid antenna. This change is linked with the increase of the transmitted power (see Section 3.3).

Others changes in the AOCS configuration are recognised in Figure 2. The two steps observed at the beginning of the plots of the CoG (see Figure 2) are due to a change in the pointing subsystem (DES reconfiguration) side B instead of side A after a depointing anomaly (see table 1 for the list of the all AOCS depointing anomaly occurred during the ERS-2 mission). The first change is from 24<sup>th</sup>, January 1996 to 14<sup>th</sup>, March 1996, the second one is from 14<sup>th</sup> February 1997 to 22<sup>nd</sup> April 1997. During these periods side B was switched on. It is important to note that during the first time a clear difference in the CoG of the received spectrum is present only for the Fore antenna (an increase of roughly 100 Hz) while during the second time the change has affected all the three antennae (roughly an increase of 200 Hz, 50 Hz and 50 Hz for the fore, mid and aft antenna respectively).

**Table 1: ERS-2 Scatterometer AOCS depointing anomaly**

From	To
24 <sup>th</sup> January 1996 9:10 a.m.	26 <sup>th</sup> January 1996 6:53 p.m.
14 <sup>th</sup> February 1997 1:25 a.m.	15 <sup>th</sup> February 1997 3:44 p.m.
3 <sup>rd</sup> June 1998 2:43 p.m.	6 <sup>th</sup> June 1998 12:47 a.m.
1 <sup>st</sup> September 1999 8:50 a.m.	2 <sup>nd</sup> September 1999 1:28 a.m.
7 <sup>th</sup> October 2000 4:38 p.m.	10 <sup>th</sup> October 2000 4:49 p.m.
24 <sup>th</sup> October 2000 4:05 p.m.	25 <sup>th</sup> October 2000 12:05 p.m.
17 <sup>th</sup> January 2001	6 <sup>th</sup> February 2001

The Figure 2 shows also when the satellite was operated in Fine Pointing Mode (FPM) in EBM, ZGM mode or the on-board doppler compensation was missing. These events are related with the large peaks in the CoG of the received spectrum plots (fore and aft antenna) and are listed in Table 2.

**Table 2: ERS-2 Scatterometer anomalies in the CoG fore and aft antenna**

Date	Reason
26 <sup>th</sup> and 27 <sup>th</sup> September 1996	missing on-board doppler coefficient (after cal. DC converter test period)
6 <sup>th</sup> and 7 <sup>th</sup> June 1998	no Yaw Steering Mode (after depointing anomaly)

Date	Reason
2 <sup>nd</sup> and 3 <sup>rd</sup> December 1998	missing on-board doppler coefficients (after AMI anomaly 228)
16 <sup>th</sup> and 17 <sup>th</sup> February 2000	Fine Pointing Mode (FPM) (due to AOCS mono-gyro qualification period)
14 <sup>th</sup> April 2000	Fine Pointing Mode (FPM)
30 <sup>th</sup> May 2000	Fine Pointing Mode (FPM)
5 <sup>th</sup> July 2000	Fine Pointing Mode (FPM) after instrument switch-on
27 <sup>th</sup> September 2000	Fine Pointing Mode (FPM) to up-load AOCS software patch
2 <sup>nd</sup> November 2000	Fine Pointing Mode (FPM)
5 <sup>th</sup> and 6 <sup>th</sup> December 2000	Fine Pointing Mode (FPM) due to orbital manoeuvre
6 <sup>th</sup> February - 30 <sup>th</sup> March 2001	Extra Backup Mode (EBM) coarse attitude control
30 <sup>th</sup> March 2001- 7th June 2001	EBM-YSM gyro-less yaw steering mode
7 <sup>th</sup> June 2001 - onwards	ZGM -YSM operations

The peaks (before February 2001) shown in the plot of mid beam standard deviation of the CoG of the received spectrum are linked to the satellite manoeuvres and AOCS depointing anomaly.

Since February 2003 (with the beta version of ESACA processor) the evolution of the Doppler compensation was stable. This because ESACA takes into account the real acquisition geometry and therefore is able to compensate for the received signal. The CoG is very close to zero and the standard deviation was reduced a lot: it was around 1800 Hz for Fore and Aft beam and around 2800 Hz for the mid beam.

During the cycle 93 the Doppler compensation evolution was very stable (see Figure 3). The small peak detected on 23rd March 2004 was due to an AOCS mode-change to FPM in order to perform an orbit manoeuvre.

## ERS-2 WindScatterometer: DOPPLER COMPENSATION Evolution (UWI)

Least-square poly. fit fore beam	Center of gravity = $-115.0 + (0.0592) \cdot \text{day}$	Standard Deviation = $4248.0 + (0.0384) \cdot \text{day}$
Least-square poly. fit mid beam	Center of gravity = $-785.2 + (0.3120) \cdot \text{day}$	Standard Deviation = $5119.9 + (0.0197) \cdot \text{day}$
Least-square poly. fit aft beam	Center of gravity = $-390.5 + (0.1748) \cdot \text{day}$	Standard Deviation = $4368.9 + (0.0272) \cdot \text{day}$

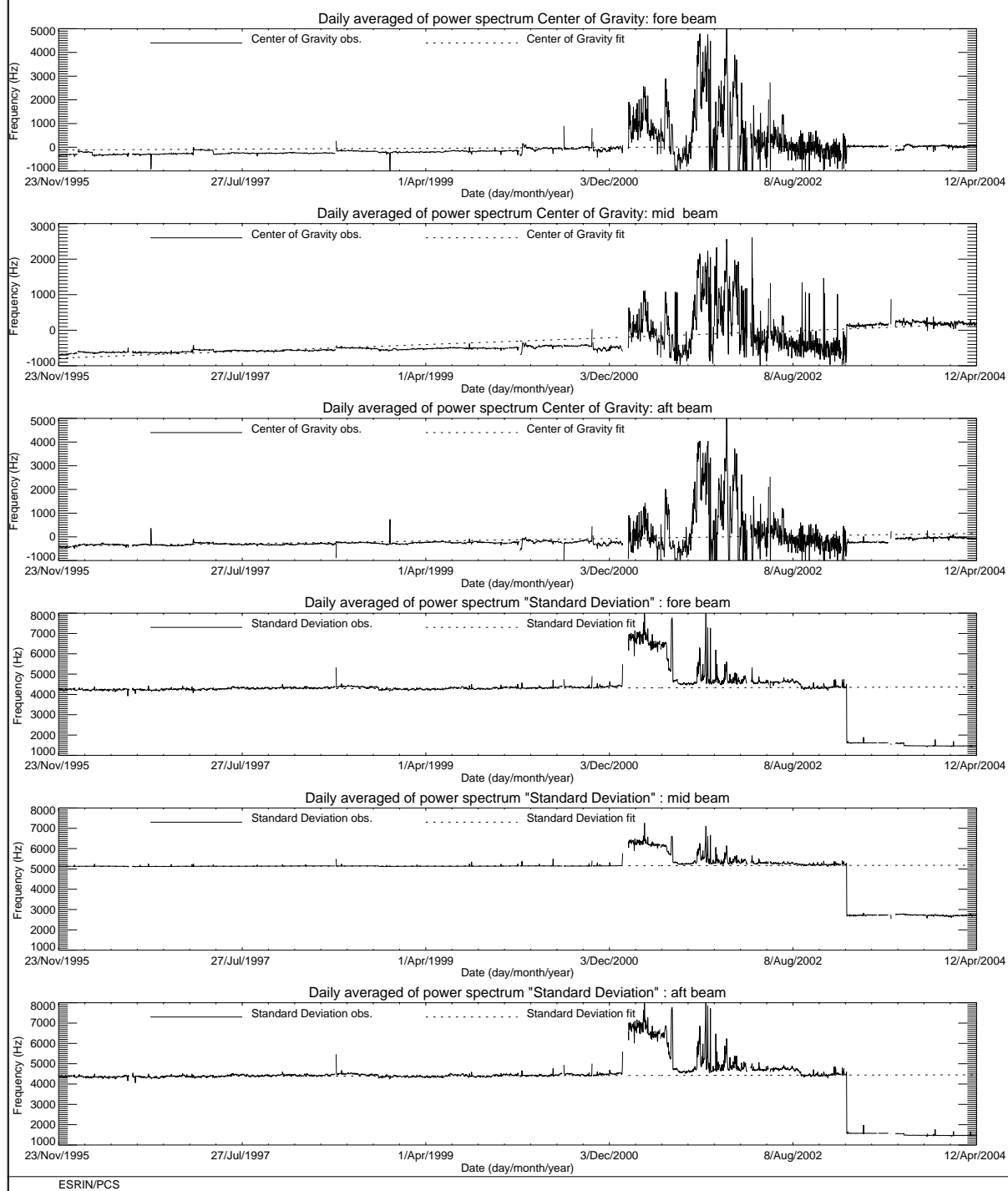


**FIGURE 2. ERS-2 Scatterometer: Centre of Gravity and standard deviation of received power spectrum since the beginning of the mission.**

## ERS-2 WindScatterometer: DOPPLER COMPENSATION Evolution (UWI)

Least-square poly. fit fore beam    Center of gravity =  $59.527 + (0.0627) \cdot \text{day}$     Standard Deviation =  $1465.5 + (0.1753) \cdot \text{day}$   
 Least-square poly. fit mid beam    Center of gravity =  $178.56 + (-0.136) \cdot \text{day}$     Standard Deviation =  $2718.1 + (-0.077) \cdot \text{day}$   
 Least-square poly. fit aft beam    Center of gravity =  $-53.54 + (-0.696) \cdot \text{day}$     Standard Deviation =  $1471.6 + (0.1097) \cdot \text{day}$

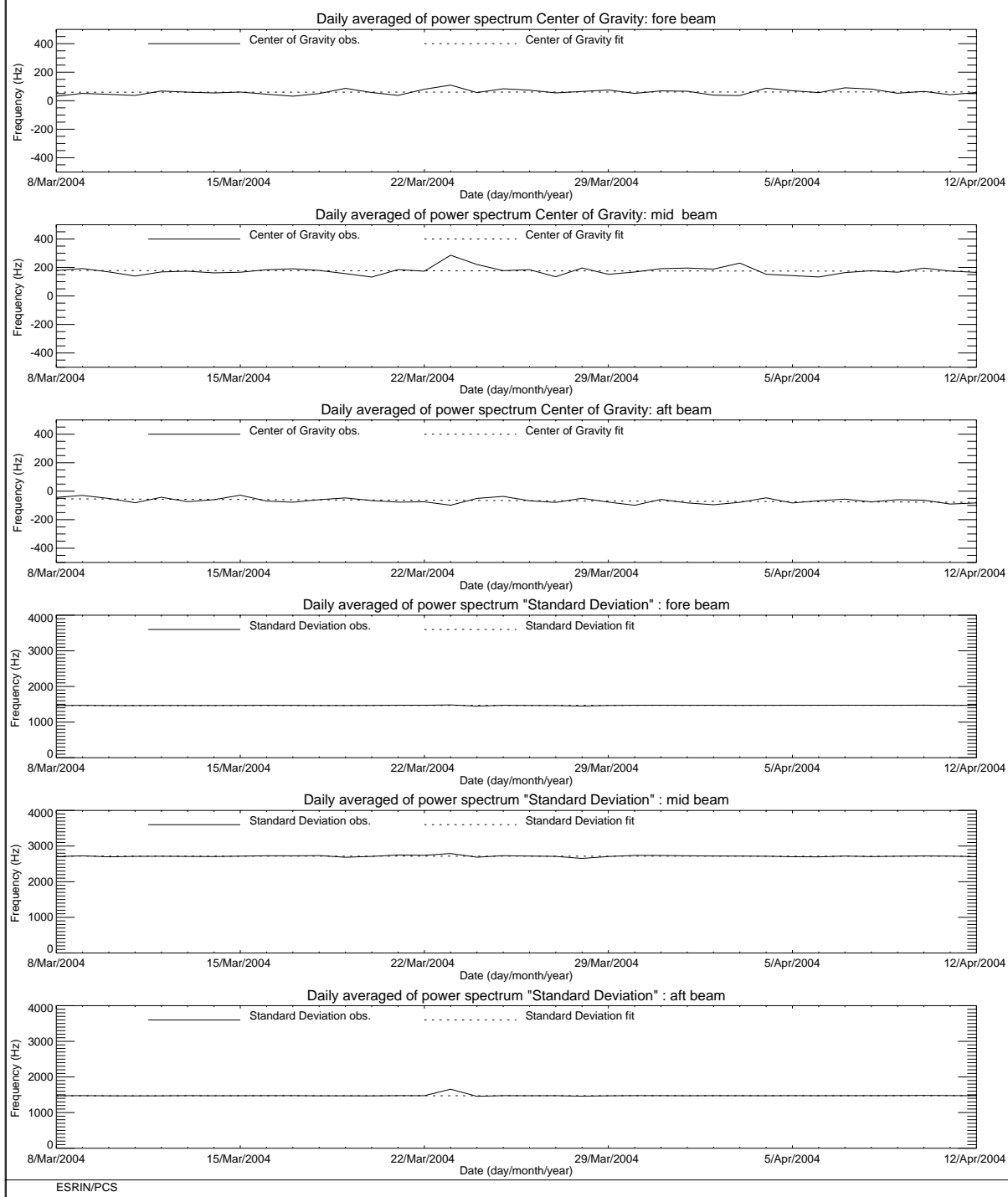


**FIGURE 3. ERS-2 Scatterometer: Centre of Gravity and standard deviation of received power spectrum during the cycle 93.**

### 3.2 Noise power level I and Q channel

The results of the monitoring are shown in Figure 4 (long-term) and Figure 5 (cycle 93). The first set of three plots presents the noise power evolution for the I channel while the second set shows the Q channel. From the plots one can see that the noise level is more stable in the I channel than in the Q one. The I and Q receivers are inside the same box and any external interference should affect both channel. The fact that the receivers are closer to the ATSR-GOMNE electronics could have some impact but there is no clear explanation on that behaviour.

From 5<sup>th</sup> December 1997 until November 1998 some high peaks appear in the plots. These high values for the daily mean are due to the presence for these special days of a single UWI product with an unrealistic value in the noise power field of its Specific Product Header. The analysis of the raw data used to generate these products lead in all cases to the presence of one source packet with a corrupted value in the noise field stored into the source packet Secondary Header. The reason why noise field corruption is beginning from 5<sup>th</sup> December 1997 and last until November 1998 is at present unknown. It is interesting to note that at the beginning of December 1997, we started to get as well the corruption of the Satellite Binary Times (SBTs) stored in the EWIC product. The impact in the fast delivery products was the production of blank products starting from the corrupted EWIC until the end of the scheduled stop time. A change in the ground station processing in March 1998 overcame this problem.

Since 9<sup>th</sup> August 1998 until March 2000 some periods with a clear instability in the noise power have been recognised. Table 3 gives the detailed list.

**Table 3: ERS-2 Scatterometer instability in the noise power**

From	To
9 <sup>th</sup> August 1998	26 <sup>th</sup> October 1998
29 <sup>th</sup> November 1998	6 <sup>th</sup> December 1998
23 <sup>rd</sup> December 1998	24 <sup>th</sup> December 1998
7 <sup>th</sup> June 1999	10 <sup>th</sup> June 1999
17 <sup>th</sup> August 1999	22 <sup>nd</sup> August 1999
8 <sup>th</sup> September 1999	9 <sup>th</sup> September 1999
3 <sup>rd</sup> October 1999	8 <sup>th</sup> October 1999
16 <sup>th</sup> October 1999	18 <sup>th</sup> October 1999
26 <sup>th</sup> October 1999	28 <sup>th</sup> October 1999
25 <sup>th</sup> December 1999	2 <sup>nd</sup> January 2000
10 <sup>th</sup> February 2000	11 <sup>th</sup> February 2000
19 <sup>th</sup> March 2000	26 <sup>th</sup> March 2000

To better understand the instability of the noise power the PCS has carried out investigations in the scatterometer raw data (EWIC) to compute the noise power with more resolution. The result is that for the orbits affected by the instability the noise power had a decrease of roughly 0.7 dB for the fore and aft signals and a decrease of roughly 0.6 dB in the mid beam case (see the report for the cycle 42).

The decrease of the noise power during the orbits affected by the instability is comparable with the decrease of the internal calibration level that occurred during the same orbits. The reason of this instability (linked to the AMI anomalies) is still under investigation.

On 28<sup>th</sup> February 2003 the Scatterometer receiver gain has been increased by 3 dB to increase the usage of the on-board ADC converter. This explains the increase of the noise for the Fore and Aft beam channel. For the mid beam channel the noise still remains not measurable.

The evolution of the noise power during the cycle 93 was stable (see Figure 5). The daily average for the Fore and Aft beam noise is around 1.7 ADC (I) and around 1.6 ADC (Q). For the Mid beam the noise is not measurable.



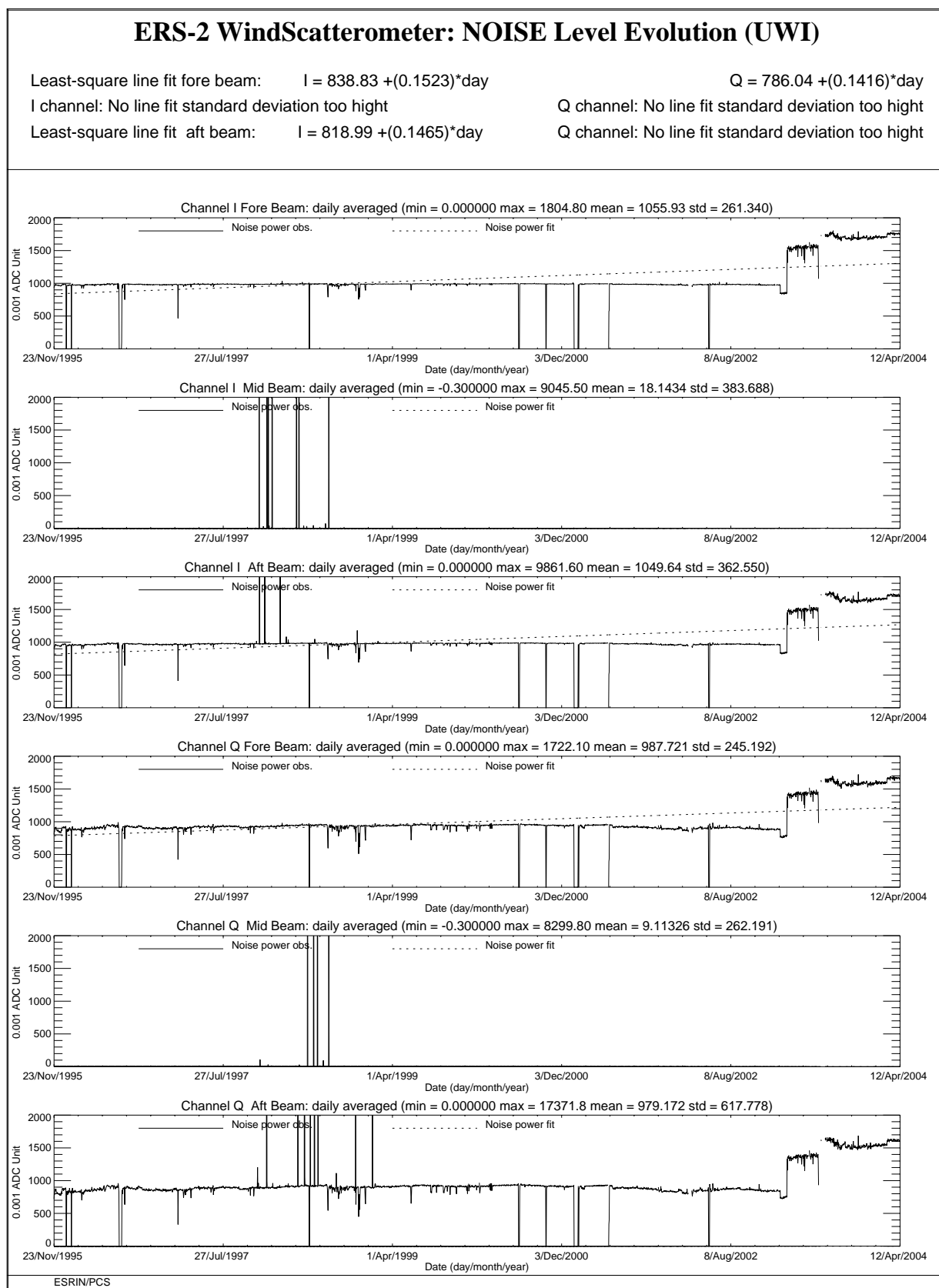


FIGURE 4. ERS-2 Scatterometer: noise power I and Q channel since the beginning of the mission.

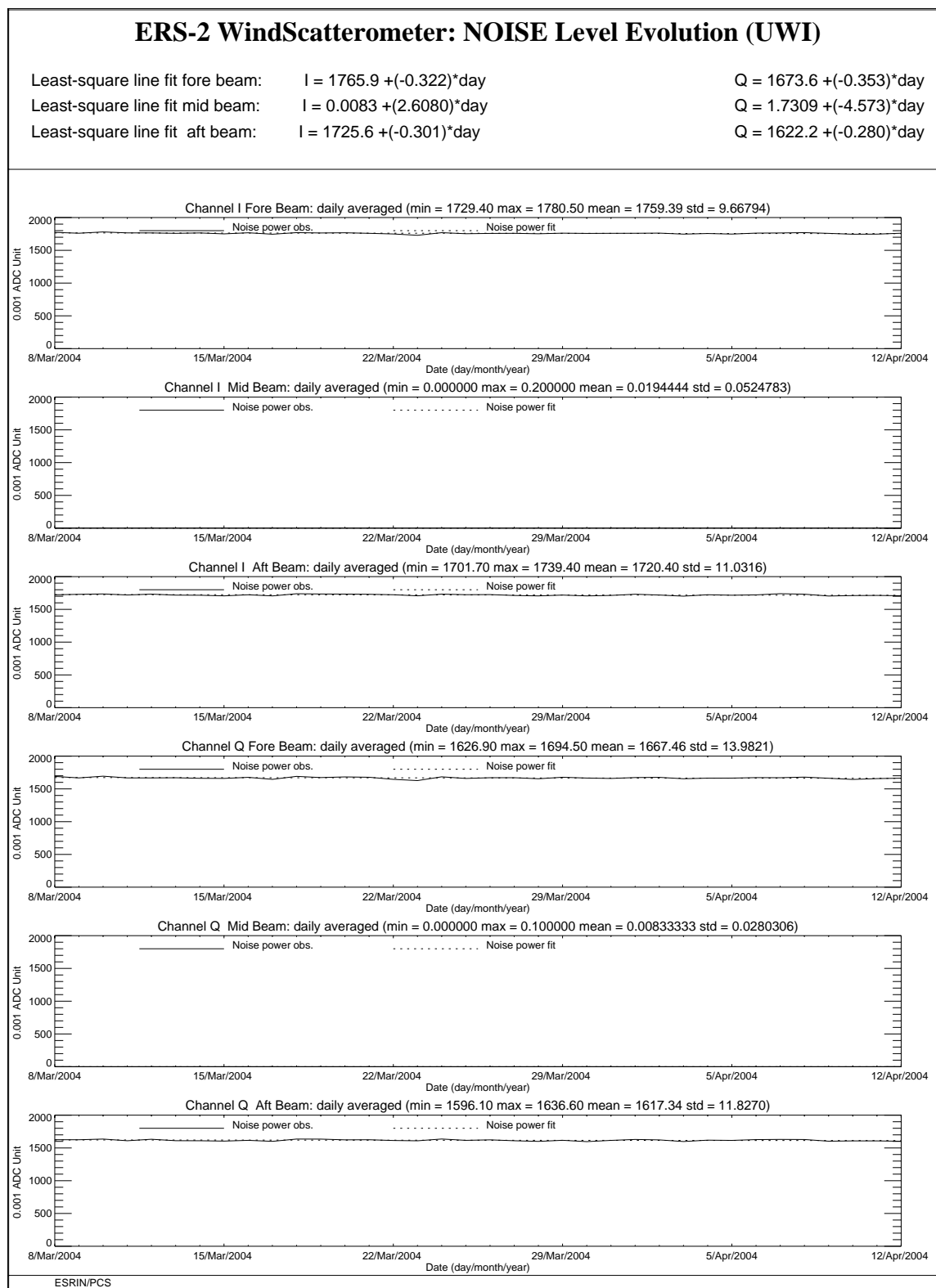


FIGURE 5. ERS-2 Scatterometer: noise power I and Q channel for cycle 93.

### 3.3 Power level of internal calibration pulse

For the internal calibration level, the results are shown in Figure 6 (long-term) and Figure 7 (cycle 93).

The high value of the variance in the fore beam until August, 12<sup>th</sup> 1996 is due to the ground processing. In fact all the blank source packets ingested by the processor were recognized as Fore beam source packets with a default value for the internal calibration level. The default value was applicable for ERS-1 and therefore was not appropriate for ERS-2 data processing. On August 12<sup>th</sup>, 1996 a change in the ground processing LUT overcame the problem.

Since the beginning of the mission a power decrease is detected. The power decrease is regular and affects the AMI when it is working in wind-only mode, wind/wave mode and image mode indifferently. The average power decrease is around 0.08 dB per cycle (0.0022 dB/day) and is more clear after August, 6<sup>th</sup> 1996 when the calibration subsystem has been changed.

The reason of the power decrease is because the TWT is not working in saturation, so that a variation in the input signal is visible in the output. The variability of the input signal can be two-fold: the evolution of the pulse generator or the tendency of the switches between the pulse generator and the TWT to reset themselves into a nominal position. These switches were set into an intermediate position in order to put into operation the scatterometer instrument (on 16<sup>th</sup> November 1995).

To compensate for this decrease, on 26<sup>th</sup> October 1998 (cycle 37) 2.0 dB were added to the Scatterometer transmitted power and on 4<sup>th</sup> September 2002 (cycle 77) were added 3.0 dB. On 28<sup>th</sup> February 2003 (cycle 82) the Scatterometer receiver gain was increased by 3 dB to improve the usage of the on-board ADC converter. These events are clearly displayed by the large steps shows in Figure 6.

Since 9<sup>th</sup> August 1998 until March 2000 the internal calibration level shows an instability after an AMI or platform anomaly (see reports from cycle 35 to cycle 52). This instability is very well correlated with the fluctuations observed in the noise power.

On 13<sup>th</sup> July 2000 an high peak (+3.5 dB) was detected in the transmitted power. This event has been investigated deeply by PCS and ESOC. The results of the analysis are reported in the technical note “ERS-2 Scatterometer: high peak in the calibration level” available in the PCS. The high transmitted power was detected after an arcing event which occurred inside the HPA. After that event the transmitted power had an average increase of roughly 0.14 dB.

During the cycle 93 the mean power decrease has been 0.04dB per cycle. That value confirm the tendency noted for the cycle 92 towards a stabilization of the transmitted power.

## ERS-2 WindScatterometer: Internal CALIBRATION Level Evolution (UWI)

Least-square polynomial fit fore beam	gain (dB) per day 0.0000	$999.113 + (0.00264145) \cdot \text{day}$
Least-square polynomial fit mid beam	gain (dB) per day 0.0000	$293.424 + (0.00186745) \cdot \text{day}$
Least-square polynomial fit aft beam	gain (dB) per day 0.0000	$980.634 + (0.00612196) \cdot \text{day}$

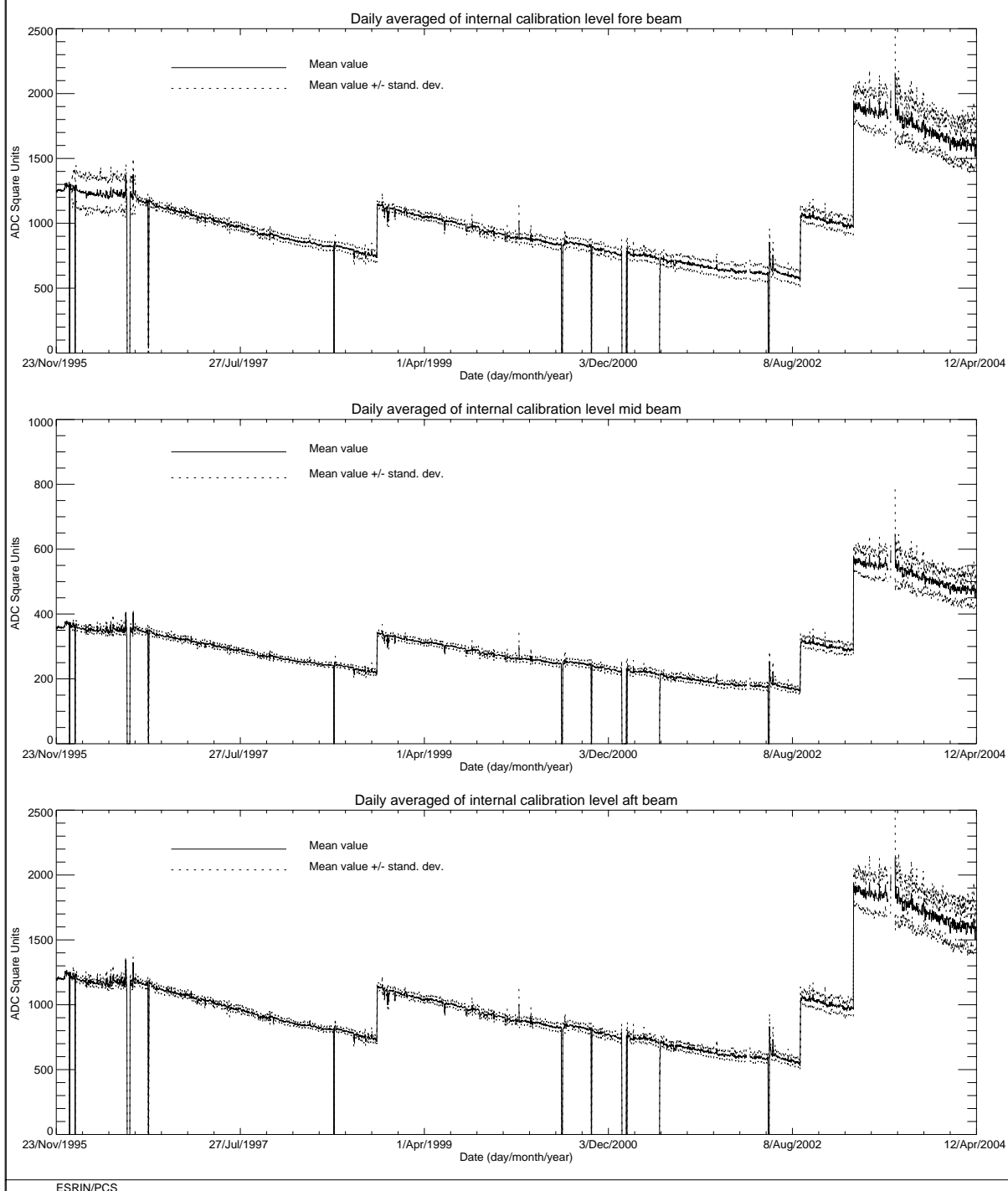


FIGURE 6. ERS-2 Scatterometer: power of internal calibration pulse since the beginning of the mission.

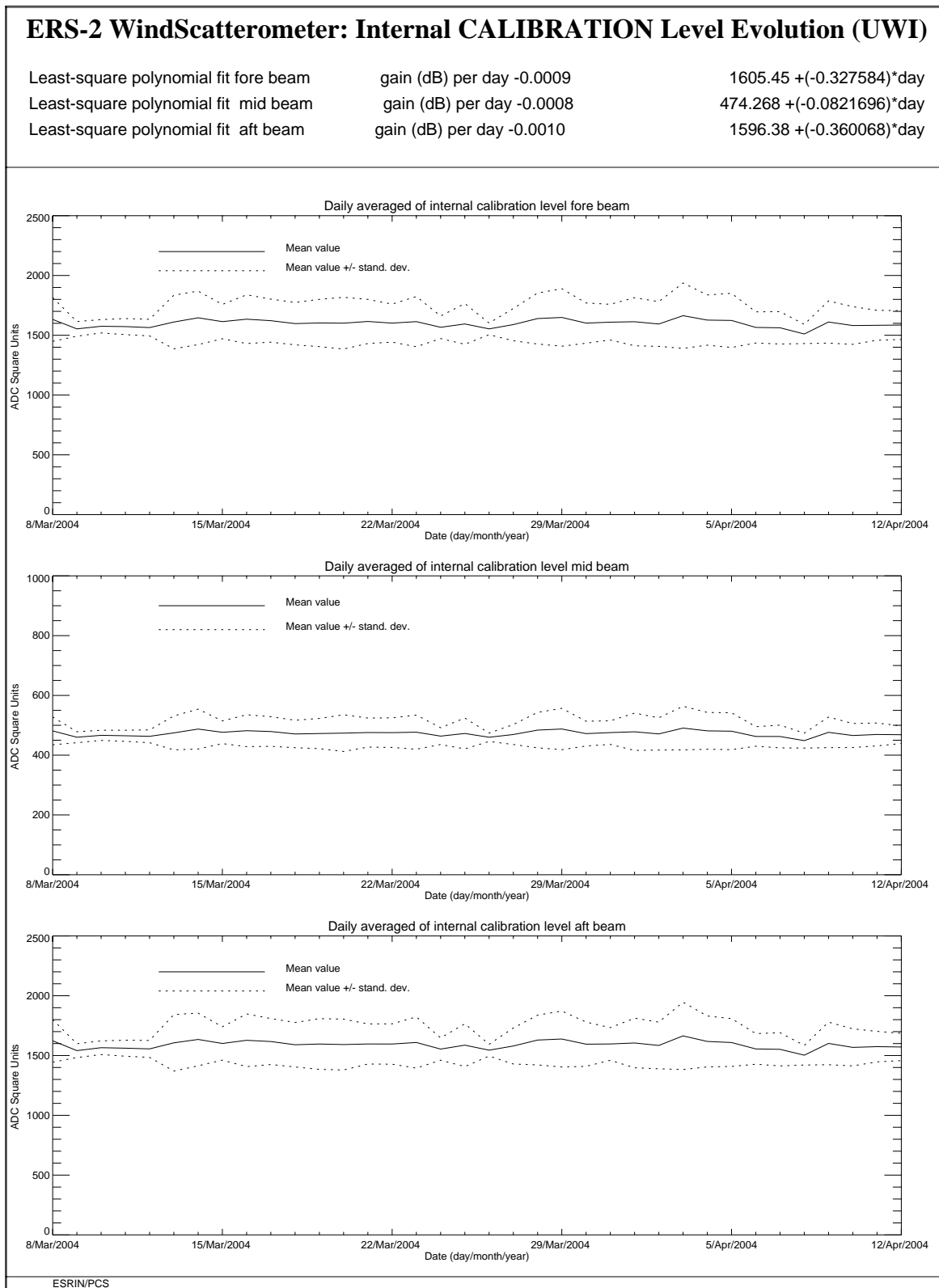


FIGURE 7. ERS-2 Scatterometer: power of internal calibration level cycle 93.

## **4.0 Products performance**

The PCS carries out a quality control of the winds generated from the WSCATT data. External contributions to this quality control (from ECMWF) are also reported in this chapter.

### **4.1 Products availability**

One of the most important point in the monitoring of the products performance is their availability. The Scatterometer is a part of ERS payload and it is combined with a Synthetic Aperture Radar (SAR) into a single Active Microwave Instrument (AMI). The SAR users requirements and the constraints imposed by the on-board hardware (e.g. amount of data that can be recorded in the on-board tape) set rules in the mission operation plan.

The principal rules that affected the Scatterometer instruments are:

- over the Ocean the AMI is in wind/wave mode (scatterometer with small SAR imagerettes acquired every 30 sec.) and the ATSR-2 is in low rate data mode.
- over the Land the AMI is in wind only mode (only scatterometer) and the ATSR-2 is in high rate mode. (Due to on board recorder capacity, ATSR-2 in high rate is not compatible with Sar wave imagerette acquisitions.)

This strategy preserves the Ocean mission.

Moreover:

- the SAR images are planned as consequence of users' request.

These rules have an impact on the Scatterometer data availability.

Since July 16<sup>th</sup> 2003 the ERS-2 Low Rate mission is continued within only the visibility of ESA ground stations over Europe, North Atlantic, the Arctic and western North America. The reason was the failure of both on-board tape recorders.

In order to maximize the data coverage, since September 7<sup>th</sup> 2003 the ground station in Maspalomas, Gatineau and Prince Albert are acquiring and processing data for all the ERS-2 satellite passes within the station visibility (apart from passes for which other satellites have an higher priority). To further increase the wind coverage of the North Atlantic area, since December 8<sup>th</sup>, 2003 is operative a new ground Station in West Freugh (UK) and data from this new station are available to the user since mid January 2004. Due to its location, the West Freugh acquisitions have some overlap with those from three other ESA stations, Kiruna, Gatineau or Maspalomas. The station overlap depends on the relative orbit of the satellite. Consequentially, overlapping wind scatterometer LBR data may be included in two products. Since the two products are generated at different ground stations the overlap may not be completely precise, with a displacement up to 12 Km and slight differences in the wind data itself.

Since 25<sup>th</sup> February 2004 onwards the ATSR is operated again in High Rate over land.

Since March, 3<sup>rd</sup> Matera station is acquiring low rate bit data for all the passes for which is planned a SAR acquisition. Gome science data are produced and disseminated to users, Radar Altimeter data, Wave data and Scatterometer data are recorded on tapes and will be available off-line

for re-processing. This means for the Scatterometer data coverage a very limited improvement due to the fact that are acquired only passes with some SAR activity.

Figure 8 shows the AMI operational modes for cycle 93. Each segment of the orbit has different colour depending on the instrument mode: brown for wind only mode, blue for wind-wave mode and green for image mode. The red and yellow colours correspond to gap modes (no data acquired).

For cycle 93 the percentage of the ERS-2 AMI activity is shown in table 4. The values are in the nominal range.

**Table 4: ERS-2 AMI activity (cycle93)**

AMI modes	ascending passes	descending passes
Wind and Wind-Wave	<b>88.8%</b>	<b>81.0%</b>
Image	<b>5.3%</b>	<b>13.9%</b>
Gap and others	<b>5.9%</b>	<b>5.1%</b>

Table 5 reports the major data lost due to the test periods, AMI and satellite anomalies or ground segment anomalies occurred after 6<sup>th</sup> August, 1996 (before that day for many times data were not acquired due to the DC converter failure).

**Table 5: ERS-2 Scatterometer mission major data lost after 6<sup>th</sup>, August 1996**

Start date	Stop date	Reason
September 23 <sup>rd</sup> , 1996	September 26 <sup>th</sup> , 1996	ERS-2 switched off due to a test period
February 14 <sup>th</sup> , 1997	February 15 <sup>th</sup> , 1997	ERS-2 switched off due to a depointing anomaly
June 3 <sup>rd</sup> , 1998	June 6 <sup>th</sup> , 1998	ERS-2 switched off due to a depointing anomaly
November 17 <sup>th</sup> , 1998	November 18 <sup>th</sup> , 1998	ERS-2 switched off to face out Leonide meteo storm
September 22 <sup>nd</sup> , 1999	September 23 <sup>rd</sup> , 1999	ERS-2 switched off due to Year 2000 certification test
November 17 <sup>th</sup> , 1999	November 18 <sup>th</sup> , 1999	ERS-2 switched off to face out Leonide meteo storm
December 31 <sup>st</sup> , 1999	January 2 <sup>nd</sup> , 2000	ERS-2 switched off Y2K transition operation
February 7 <sup>th</sup> , 2000	February 9 <sup>th</sup> , 2000	ERS-2 switched off due to new AOCS s/w up-link
June 30 <sup>th</sup> , 2000	July 5 <sup>th</sup> , 2000	ERS-2 Payload switched-off after RA anomaly
July 10 <sup>th</sup> , 2000	July 11 <sup>th</sup> , 2000	ERS-2 Payload reconfiguration
October 7 <sup>th</sup> , 2000	October 10 <sup>th</sup> , 2000	ERS-2 Payload switched-off after AOCS anomaly
January 17 <sup>th</sup> , 2001	February 5 <sup>th</sup> , 2001	ERS-2 Payload switched-off due to AOCS anomaly
May 22 <sup>nd</sup> , 2001	May 24 <sup>th</sup> , 2001	ERS-2 Payload switched-off due to platform anomaly
May 25 <sup>th</sup> , 2001	May 25 <sup>th</sup> , 2001	AMI switched-off due thermal analysis
November 17 <sup>th</sup> , 2001	November 18 <sup>th</sup> , 2001	ERS-2 switched off to face out Leonide meteo storm
November 27 <sup>th</sup> , 2001	November 28 <sup>th</sup> , 2001	ERS-2 payload off due to 1Gyro Coarse Mode commissioning
March 8 <sup>th</sup> , 2002	March 20 <sup>th</sup> , 2002	ERS-2 payload unavailability after RA anomaly



Start date	Stop date	Reason
May 19 <sup>th</sup> , 2002	May 24 <sup>th</sup> , 2002	AMI switched-off due to arc events
May 24 <sup>th</sup> , 2002	May 28 <sup>th</sup> , 2002	AMI partially switched-off due to arc events
May 31 <sup>st</sup> , 2002	June 3 <sup>rd</sup> , 2002	Gatineau orbits partially acquired due to antenna problem
June 4 <sup>th</sup> , 2002	June 5 <sup>th</sup> , 2002	AMI partially switched-off due to arc events
July 25 <sup>th</sup> , 2002	July 25 <sup>th</sup> , 2002	AMI switched off HPA voltage too low
September 11 <sup>th</sup> , 2002	September 11 <sup>th</sup> , 2002	AMI switched off macrocommand transfer error
November 17 <sup>th</sup> , 2002	November 18 <sup>th</sup> , 2002	ERS-2 switched off to face out Leonide meteo storm
December 9 <sup>th</sup> , 2002	December 10 <sup>th</sup> , 2002	IDHT anomaly no data recorded on board
December 20 <sup>th</sup> , 2002	December 20 <sup>th</sup> , 2002	IDHT anomaly no data recorded on board
January 14 <sup>th</sup> , 2003	January 14 <sup>th</sup> , 2003	IDHT anomaly no data recorded on board
16 <sup>th</sup> May 2003	19 <sup>th</sup> May 2003	AMI off due to bus reconfiguration
June 22 <sup>nd</sup> , 2003	July 16 <sup>th</sup> , 2003	IDHT recorders test no data acquired
July 16 <sup>th</sup> , 2003	onwards	Data available only within the visibility of ESA ground station

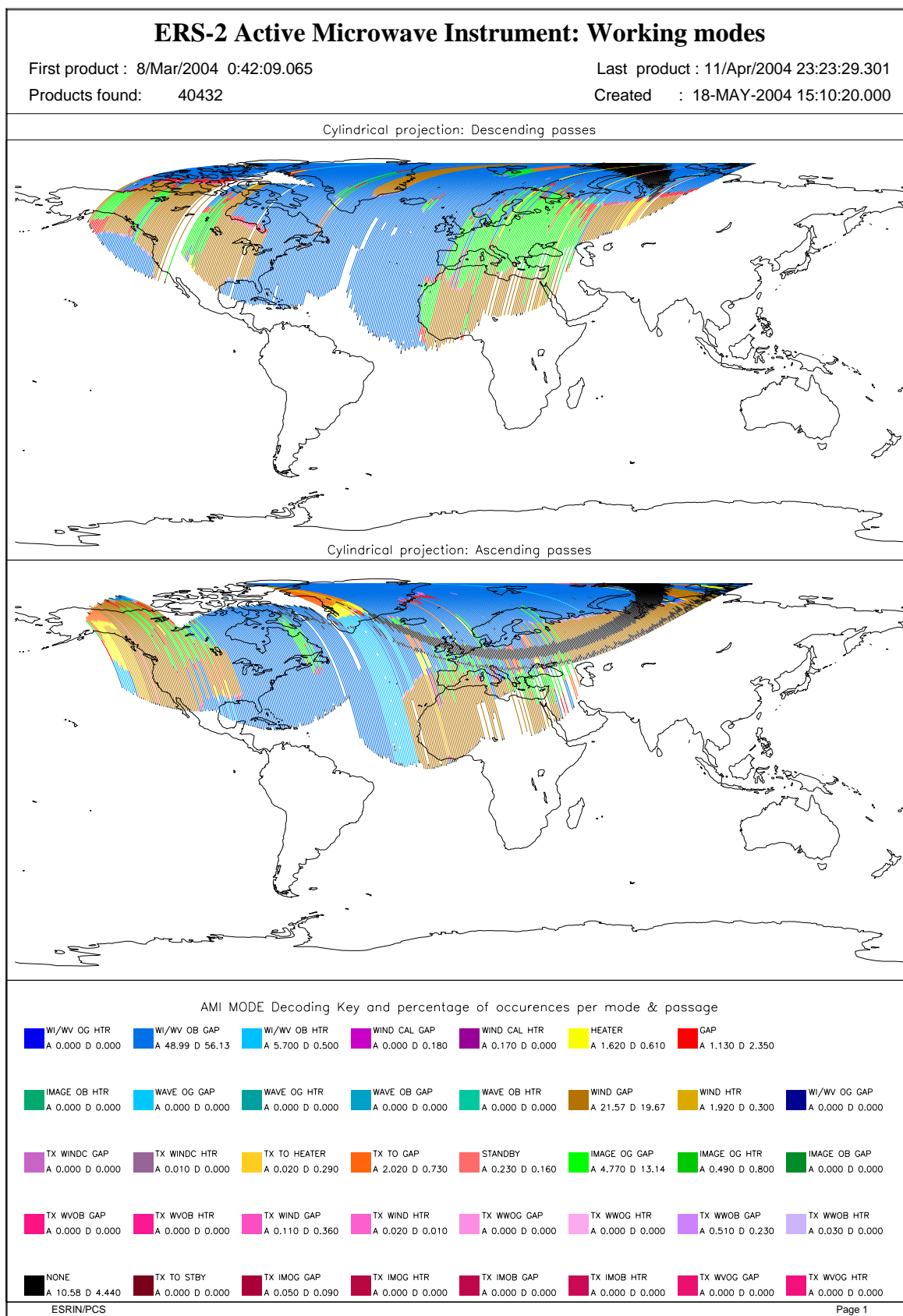


FIGURE 8. ERS-2 AMI activity during cycle 93.

## 4.2 PCS Geophysical Monitoring

The routine analysis is summarized in the plots of figure 9; from top to bottom:

- the monitoring of the valid sigma-nought triplets per day.
- the evolution of the wind direction quality. The ERS wind direction (for all nodes and only for those nodes where the ambiguity removal has worked properly) is compared with the ECMWF forecast. The plot shows the percentage of nodes for which the difference falls in the range -90.0, +90.0 degrees.
- the monitoring of the percentage of nodes whose ambiguity removal works successfully.
- the comparison of the wind speed deviation: (bias and standard deviation) with the ECMWF forecast.

The results since August 6<sup>th</sup>, 1996 until the beginning of the operation with the Zero Gyro Mode (ZGM) in January 2001 can be summarized as:

- High quality wind products has been distributed since Mid March 1996 (end of calibration and validation phase)
- The number of valid sigma-nought distributed per day was almost stable with a small increase after June 29<sup>th</sup>, 1999 due to the dissemination in fast delivery of the data acquired in the Prince Albert station.
- The wind direction is very accurate for roughly 93% of the nodes, the ambiguity removal processing successfully worked for more than 90.0% of the nodes.
- The UWI wind speed shows an absolute bias of roughly 0.5 m/s and a standard deviation that ranges from 2.5 m/s to 3.5 m/s with respect to the ECMWF forecast.
- The wind speed bias and its standard deviation have a seasonal pattern due to the different winds distribution between the winter and summer season.
- Two important changes affect the speed bias plot.
- the first is on June 3<sup>rd</sup>, 1996 due to the switch from ERS-1 to ERS-2 data assimilation in the meteorological model.
- the second which occurred at the beginning of September 1997, is due to the new monitoring and assimilation scheme in ECMWF algorithms (4D-Var).
- Since 19<sup>th</sup> April 1999 two set of meteo-table (meteorological forecast centred at 00:00 and 12:00 of each day) are used in the ground processing. This allowed the processing of wind data with 18 and 24 hours meteorological forecast instead of the 18, 24, 30 36 hours forecast. The comparison between data processed with the 18-24 hours forecast instead of 30-36 hours forecast shown an increase in the number of ambiguity removed nodes with a neutral impact in the daily statistics.
- The mono-gyro AOCS configuration (see report for cycle 50) that was operative from 7<sup>th</sup> February 2000 to 17<sup>th</sup> January 2001 did not affect the wind data performance.

During the Zero Gyro Mode (ZGM) phase the dissemination of the fast delivery scatterometer data to the users has been interrupted on 17<sup>th</sup> January 2001 due to degraded quality in sigma noughts and winds. The satellite attitude in ZGM is slightly degraded and the “old” ground processor was not able to produce calibrated data anymore. For that reason a re-design of the entire

ground processing has been carried out and since August 21<sup>st</sup> 2003 the new processor named ERS Scatterometer Attitude Corrected Algorithm (ESACA) is operative in all the ESA ground station and data was redistributed to the user.

Although for a long period data was not distributed, the PCS has monitored the data quality (as shown in Figure 9) and the results during that period can be summarized as:

At the beginning of the ZGM (January 2001 - end July 2001) the number of valid nodes has a clear drop from 190000 per day to 9000 per day. This because the satellite attitude was strongly degraded and the received signal had a very high Kp figure (in particular for the far range nodes). For the valid nodes, due to no calibrated sigma nought, the quality of the wind was very poor, the distance from the cone was high and the wind speed bias was above 1.5 m/s.

At the end of July 2001 the ZGM has been tuned and the satellite attitude had an improvement. This explains the increase of the number of valid nodes (returned around the nominal level) and the improvements in the wind speed bias (around 0.5 m/s).

On 4<sup>th</sup> February 2003, a beta version of the new ESACA processor has been put in operation in Kiruna for validation and the monitoring of the data quality has been done only for the new ESACA data. The number of valid nodes slightly decreased because Kiruna station processes only 9 of 14 orbits per day. The wind speed direction deviation had a clear improvement because ESACA implements a new ambiguity removal algorithm (MSC) and the ambiguity removal rate is now stable at 100% (the MSC is able to remove ambiguity for all the nodes). The wind speed bias had a clear drop from 0.5 to -0.5 m/s. That value is closer to the nominal one (around -0.2 m/s). As reported in the previous cyclic reports the beta version of ESACA had some calibration problem for the near range nodes and this explains why the data quality does not match exactly the one obtained in the nominal YSM. That problem has been overcome with the final release of the ESACA processor put into operation on August 21<sup>st</sup> 2003.

On June 22<sup>nd</sup> the failure of the on-board tape recorder discontinued the ERS global mission (see section 4.1) and this explains the low number of valid nodes available after that day.

Currently the performances of ESACA winds are affected by land contamination. Around coastal zones many Sea nodes have a strong contribution of Land backscattering and the retrieved wind is not correct. An optimization of the Land/Sea flag in the ground processing is under implementation.

In the statistics computed by PCS on the fast delivered winds the Land contamination has been removed by using a refined Land/Sea mask. Also the ice contamination has been removed with a simple geographical filter. With these new settings the PCS statistics are very similar to the ones reported by ECMWF.

For cycle 93 the wind speed bias (UWI vs 18 or 24 hour forecast) is roughly 0.5 m/s and the speed bias standard deviation is around 1.5 m/s. The fluctuation of the statistics is mainly due to the small amount of data available for each day.

The wind direction deviation has improved. Roughly the 98% (it was 96% for cycle 92) of the nodes have a wind direction in agreement with the meteorological forecast.

Performances of ESACA winds computed by ECMWF are given in section 4.3.

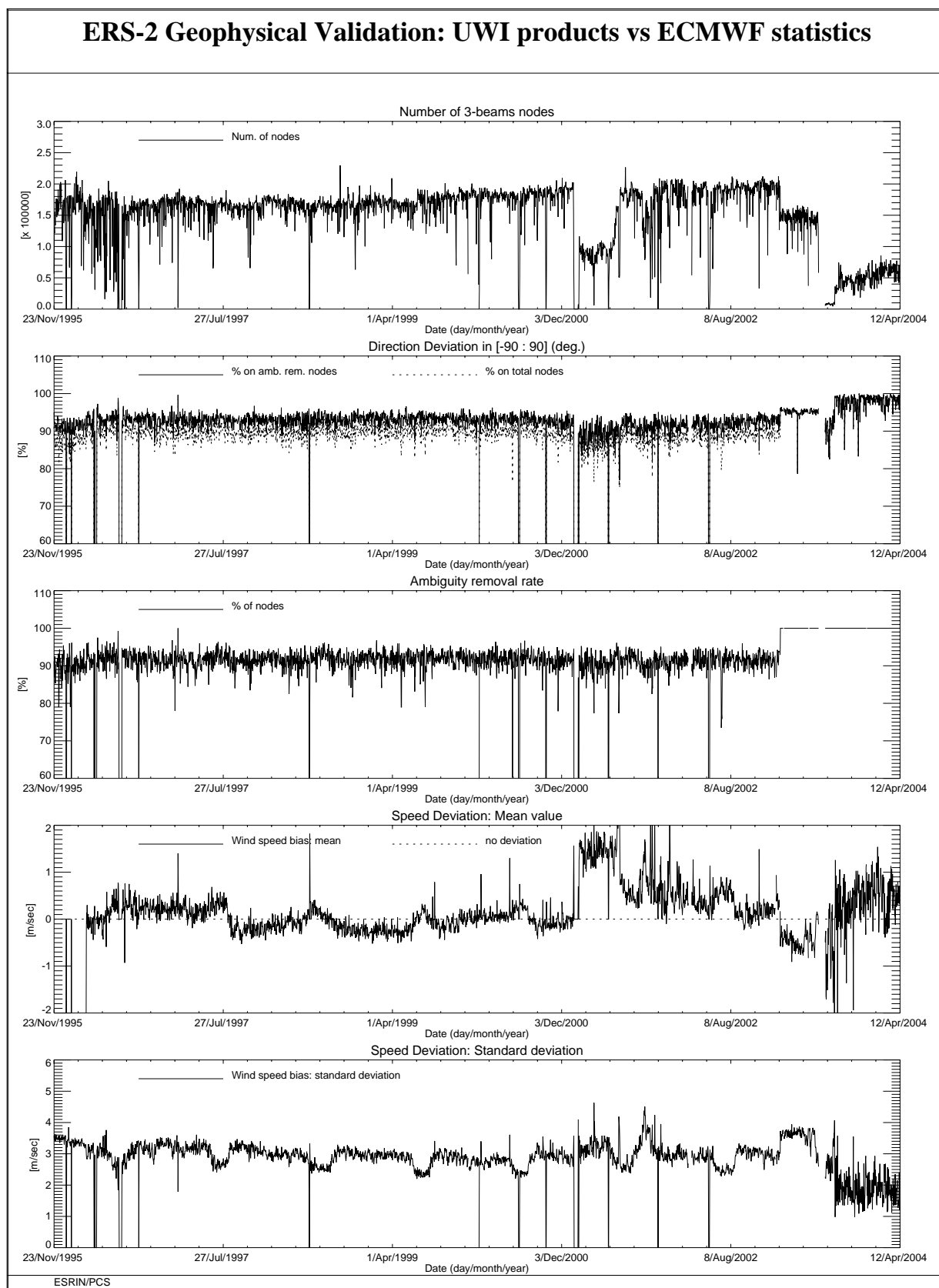


**FIGURE 9. ERS-2 Scatterometer: wind products performance since the beginning of the mission.**

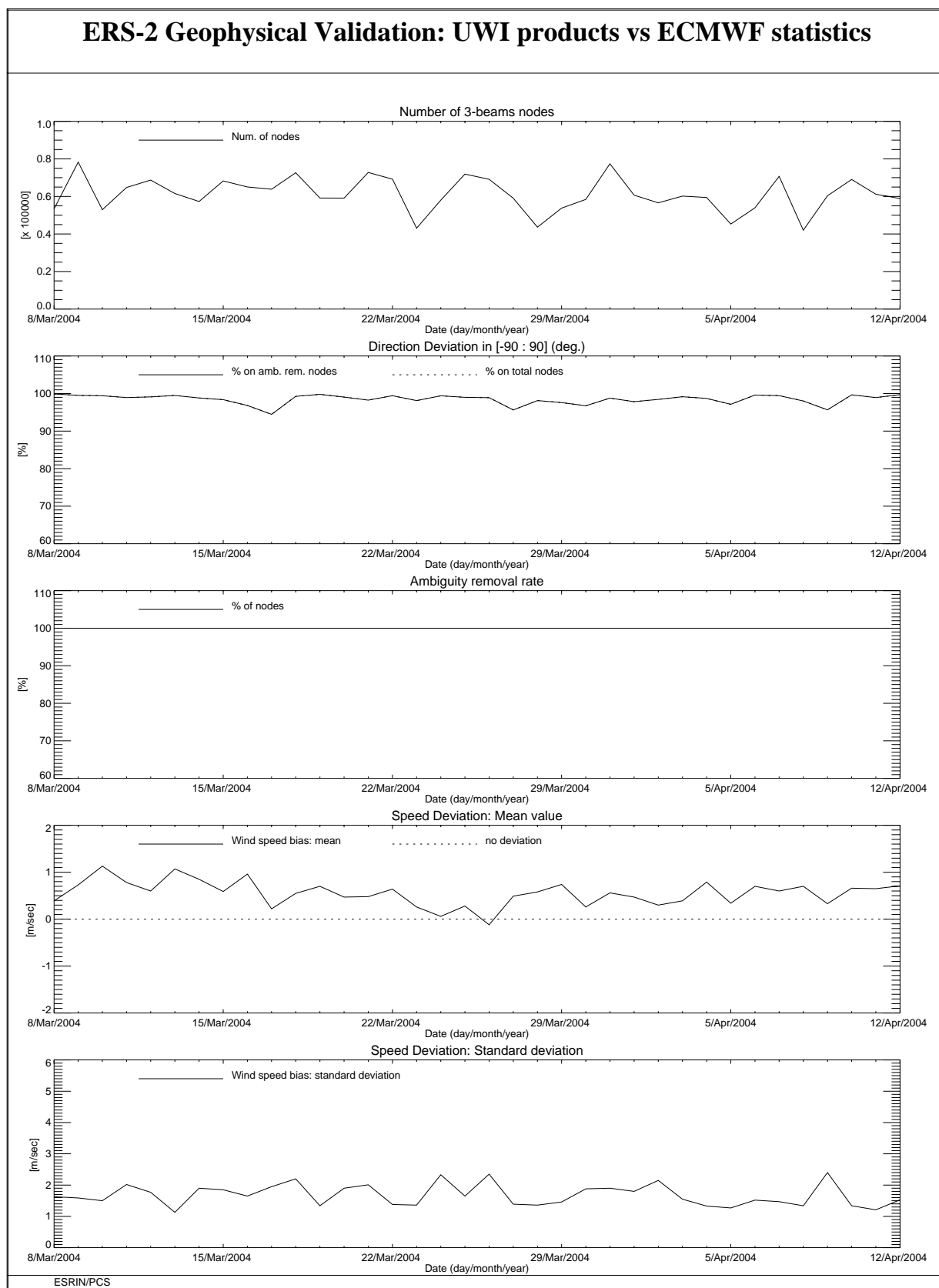
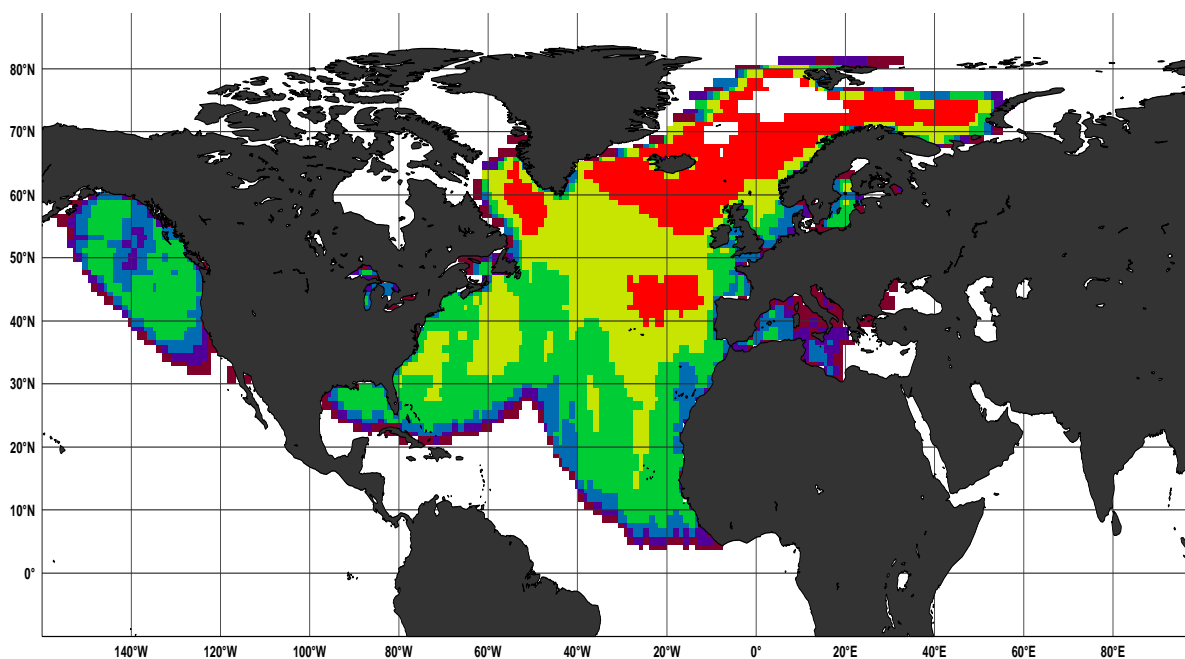


FIGURE 10. ERS-2 Scatterometer: wind products performance for cycle 93.

### 4.3 ECMWF Geophysical Monitoring

On 21 August 2003, the world-wide dissemination of ERS-2 data was restarted. Due to a failure of both on-board LBR tape recorders two months earlier, only data is being received for data within the visibility range of a ground station. In practice this limits coverage to the North-Atlantic, part of the Mediterranean, the Gulf of Mexico, and to a small part of the Pacific north-west from the US and Canada (see Figure 11). Since 8<sup>th</sup> December 2003, a new ground station became operational at West Freugh (Scotland, UK), filling the gap in data coverage over the North-Atlantic. However, at ECMWF, data for this station was only received from 23:47 UTC 15 January 2004 onwards. Its area of coverage, with the exception of the previously existing gap, is now reported by more than one ground station, which leads to a duplication in dissemination. Locations of vector wind cells between stations can differ up to 12km. The UWI winds are mostly almost identical, however, the result of the de-aliasing is occasionally not equal, resulting in anti-parallel winds (Note from ESRIN: for each node the ambiguity removal is performed taking into account a large area of influence around the node. It happens that for the same node the area of influence differs from one station to other due to the data acquisition strategy. Differences in the area of influence explains the result reported by ECMWF. ESRIN is investigating the possibility to centralize the Scatterometer data processing in order to remove dissemination of duplicated winds



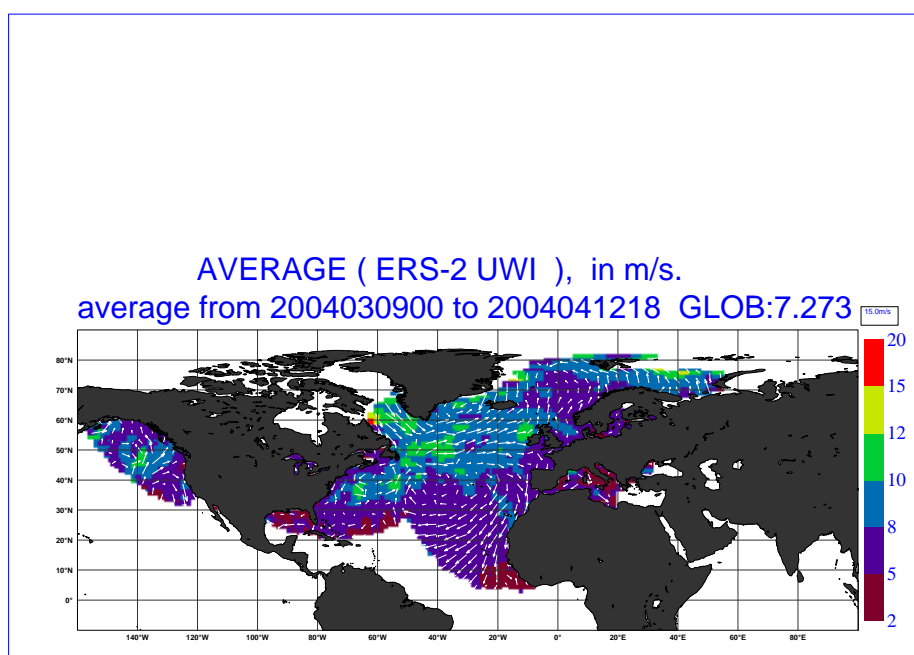
**FIGURE 11.** Average number of observations per 12H and per 125km grid box for UWI winds that passed the UWI flags QC and a check on the collocated ECMWF land and sea-ice mask.

For the entire period in cycle 93, ERS-2 scatterometer data was used in the 4D-Var data assimilation system at ECMWF. The re-introduction of the UWI data occurred just prior to the start of cycle 93, and makes now use of CMOD5-based winds. Since cycle 59 in January 2001, this is the first 5-weekly period for which UWI data was assimilated at ECMWF.

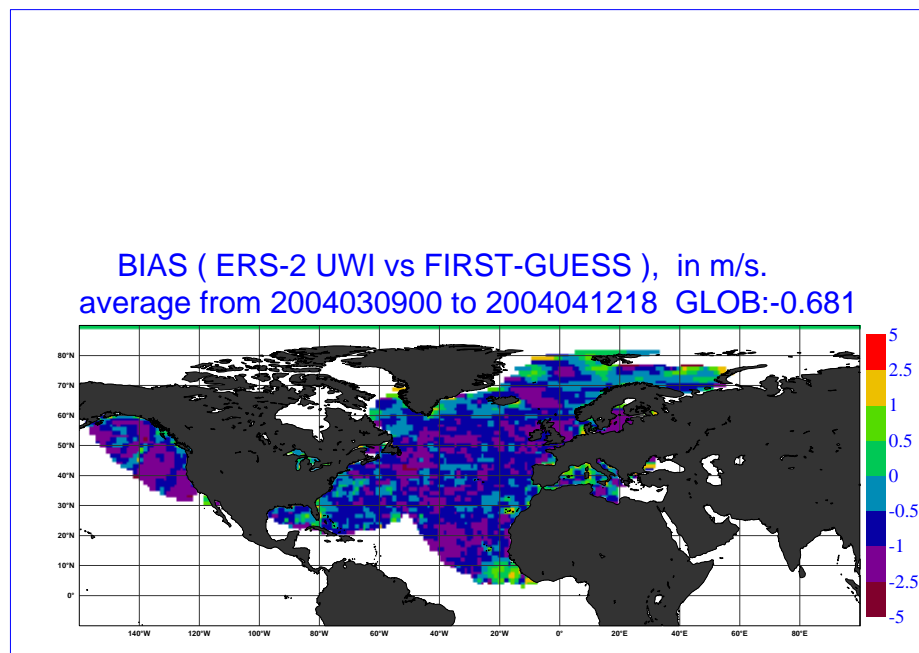
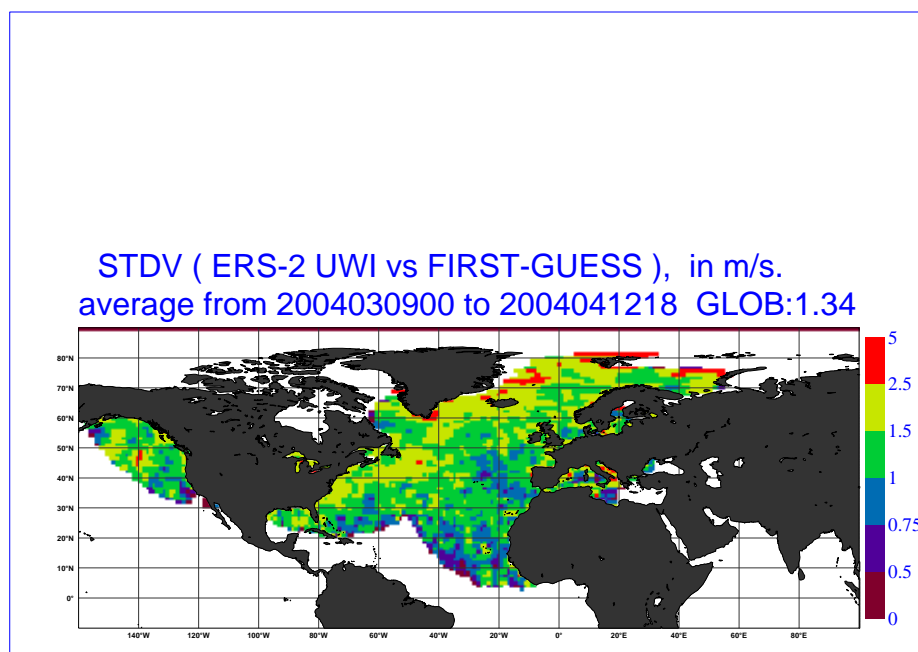
The quality of the UWI product was monitored at ECMWF for cycle 93. Results were compared to those obtained from the previous cycle, as well for data received during the nominal period in 2000 (up to cycle 59). No corrections for duplicate observations were applied.



During cycle 93, data was received between 21:06 UTC 8 March 2004 and 20:59 UTC 12 April 2004. Data was received for all 6-hourly batches, however, for 06 UTC 24 March 2004 and 06 UTC 08 April 2004 very low amounts were recorded (Note from ESRIN on 8 April it was due to an AMI anomaly occurred on that day). Mostly, the asymmetry between fore and aft incidence angles was within bounds (3 degrees). A few peaks occurred, the largest (6 degrees) around 00 UTC 24 March 2004, 12 UTC 28 March 2004 and 15 UTC 4 April 2004, for which none of them seemed to be linked to enhanced solar activity (Note from ESRIN: on 23 and 28 March 2004 a planned manoeuvres occurred with a degradation of the satellite attitude. This fact explains some of the peaks reported by ECMWF. Others peaks are related with strong degradation in the yaw angle). Compared to cycle 92, the agreement with ECMWF first-guess (FGAT) fields has improved with regard to relative standard deviation (from 1.67 m/s to 1.54 m/s). However, the relative bias has become larger (from -0.51 m/s to -0.70 m/s). A small part of the reduced random deviations is expected to result from the re-introduction of UWI data in the assimilation system. However, the impact on the monitor statistics would have been larger if ECMWF analysis winds would have been used, rather than FGAT. Another, probably larger part of the reduction, must originate from the seasonal trend of the regional data set, which makes an objective judgment on the quality of the UWI product difficult. The larger negative bias of the UWI winds seems more objective. This conjecture is confirmed by a similar trend in the backscatter levels. Both standard deviations and bias levels of wind speed are better to those for 2000. The quality of both UWI and de-aliased CMOD4 wind direction has improved. As stated above, the ECMWF assimilation system was not changed during cycle 93, though just before the start of this period (for details see report for cycle 92).



**UWI mean wind speed and direction cycle 93**

**UWI wind speed bias cycle 93****UWI wind speed standard deviation cycle 93**

### 4.3.1 Distance to cone history

The distance to the cone history is shown in Figure 12.

Curves are based on data that passed all QC, including the test on the k<sub>p</sub>-yaw flag, however subject to the land and sea-ice check at ECMWF (see cyclic report 88 for details). Like for cycle 92, time series are (due to lack of statistics) very noisy, especially for the first nodes. This makes it difficult to identify peaks that might indicate a low data quality. Most spikes are a result from low data volumes. Compared to cycle 92, average levels were slightly reduced from 1.21 to 1.19 and are now about 9% higher than for nominal data

### 4.3.2 UWI minus First-Guess history

In Figure 13, the UWI minus ECMWF first-guess wind-speed history is plotted.

The history plot shows many peaks. Most peaks are a result of low data volume. Other peaks do indicate a real discrepancy between UWI and ECMWF winds, such as for 18 UTC 9 April 2004. For this period, the area of largest disagreement, occurring north-west of Norway. It indicates a small misplacement of a (polar?) low, with sharp gradients in wind speed. Besides from some problems in the de-aliasing, the UWI winds look realistic. In the analysis, having used the scat data, the position of the low was corrected.

Similar results apply for the history of de-aliased CMOD4 winds versus FGAT (Figure 14).

Average bias levels and standard deviations of UWI winds relative to FGAT winds are displayed in Table 6.

**Table 6: Biases and standard deviation of ERS-2 versus ECMWF FGAT winds in m/s for speed and degrees for direction**

	Cycle 92 UWI	Cycle 92 CMOD-4	Cycle 93 UWI	Cycle 93 CMOD-4
speed stdev	1.67	1.65	1.54	1.53
node 1-2	1.74	1.69	1.61	1.58
node 3-4	1.67	1.64	1.51	1.50
node 5-7	1.58	1.57	1.47	1.46
node 8-10	1.61	1.60	1.47	1.47
node 11-14	1.63	1.62	1.50	1.49
node 15-19	1.65	1.65	1.54	1.54
speed bias	-0.51	-0.49	-0.70	-0.69
node 1-2	-1.13	-1.08	-1.31	-1.28
node 3-4	-0.79	-0.72	-1.01	-0.96
node 5-7	-0.52	-0.48	-0.74	-0.71
node 8-10	-0.37	-0.36	-0.54	-0.54
node 11-14	-0.33	-0.32	-0.52	-0.52

**Table 6: Biases and standard deviation of ERS-2 versus ECMWF FGAT winds in m/s for speed and degrees for direction**

	Cycle 92 UWI	Cycle 92 CMOD-4	Cycle 93 UWI	Cycle 93 CMOD-4
node 15-19	-0.28	-0.27	-0.47	-0.48
direction stdev	34.3	19.7	26.9	18.2
direction bias	-2.8	-2.8	-2.8	-2.8

From this it is seen that the bias of both the UWI and CMOD4 product have become more negative by 0.2 m/s. Biases are most negative in the near range (-1.3 m/s, see also third panel of Figure 1). The average bias level is still less negative than for nominal data in 2000 (UWI: -0.70 m/s now, was -0.79 m/s for cycle 59). In order to investigate whether the increasing bias is connected to the ECMWF model change, a time series over cycles 91 to 93 of QuikSCAT winds versus FGAT winds has been produced (not included in this report). It shows that there is no global trend in the level of the FGAT winds. To check whether the increased bias could be a result of the change of the regional wind-climate in combination with known wind-speed dependent biases of CMOD4, a time series for CMOD5 winds is computed. It does confirm the development of a bias, although, compared to cycle 91, the trend is smaller. The standard deviation of UWI winds compared to cycle 92 has improved substantially (1.54 m/s, was 1.67 m/s). The improvement as function of incidence angle is reasonably homogeneous. Performance is, like for cycles 92 and 91 (but not like cycle 90 and before) worst in the near range. For cycle 93 the (UWI - FGAT) direction standard deviations were ranging between 20 and 40 degrees. Sharp peaks are the result of low data volumes. For de-aliased CMOD4 winds values between 20 and 30 degrees are most common.

### 4.3.3 Scatter plots

Scatterplots of model 10 m first-guess winds versus ERS-2 winds are displayed in Figures 17 to 19. Values of standard deviations and biases are slightly different from those displayed in Table 6. Reason for this is that, for plotting purposes, the in 0.5 m/s resolution ERS-2 winds have been slightly perturbed (increases scatter with 0.02 m/s), and that zero wind-speed ERS-2 winds have been excluded (decreases scatter with about 0.05 m/s). The scatterplot of UWI wind speed versus FGAT is very similar to that for (at ECMWF inverted) de-aliased CMOD4 winds. It confirms that the ESACA inversion scheme is working properly. The reduced standard deviation compared to cycle 92 (1.56 m/s, was 1.68 m/s), seems to originate from a better agreement at strong winds between 15 and 20 m/s. Winds derived on the basis of CMOD5 are displayed in Figure 20. The bias compared to FGAT winds remains small for all wind domains (on average -0.15 m/s, was 0.06 m/s). The relative standard deviation is lower than for CMOD4 winds (1.50 m/s versus 1.56 m/s).

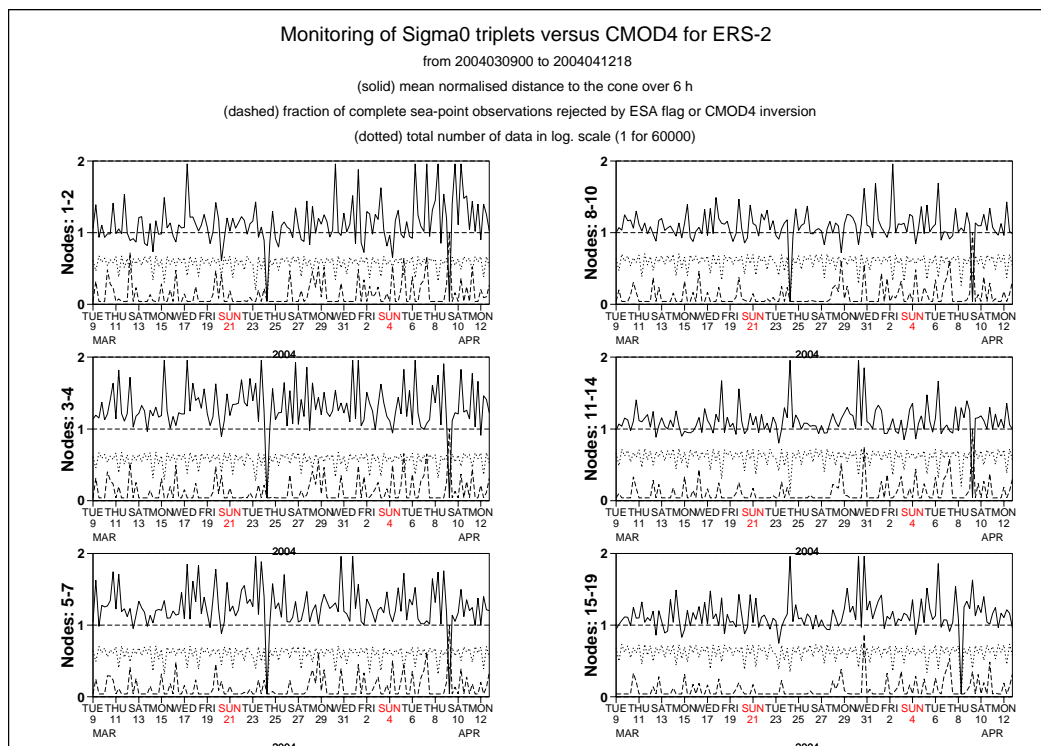


**FIGURE 12.** Mean normalised distance to the cone computed every 6 hours for nodes 1-2, 3-4, 5-7, 8-10, 11-14 and 15-19 (solid curve close to 1 when no instrumental problems are present). The dotted curve shows the number of incoming triplets in logarithmic scale (1 corresponds to 60,000 triplets) and the dashed one indicates the fraction of complete sea-located triplets rejected by the ESA flag, or by the wind inversion algorithm (0: all data kept, 1: no data kept). Cycle 93

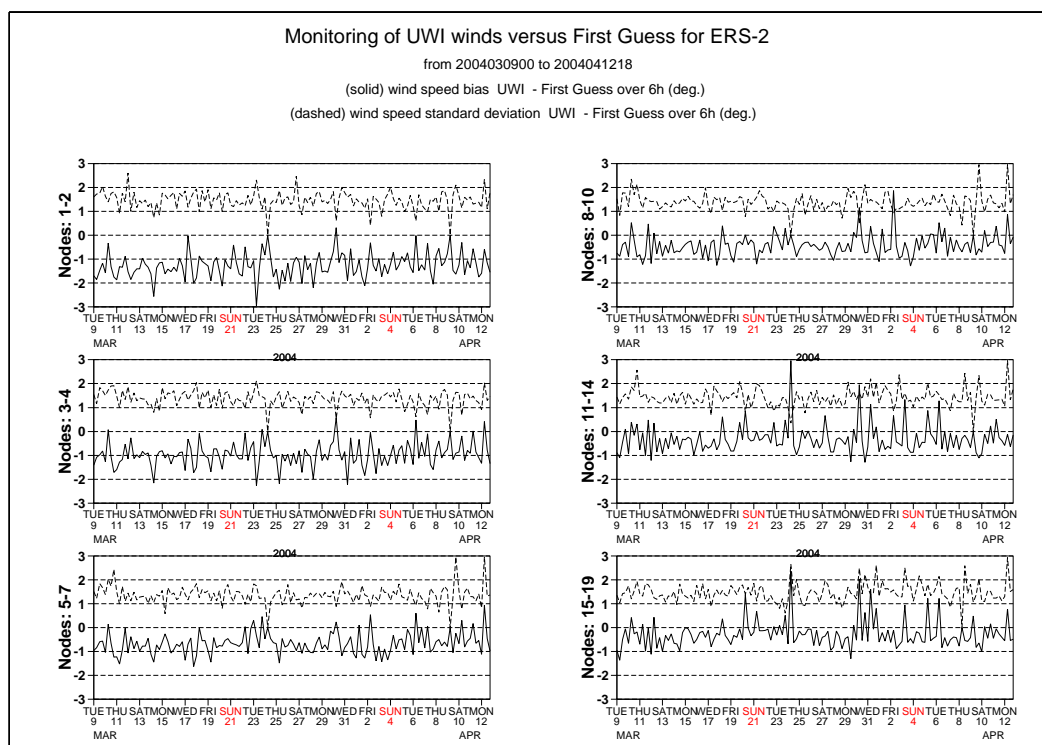


**FIGURE 13.** Mean (solid line) and standard deviation (dashed line) of the wind speed difference UWI - first guess for the data retained by the quality control.Cycle 93

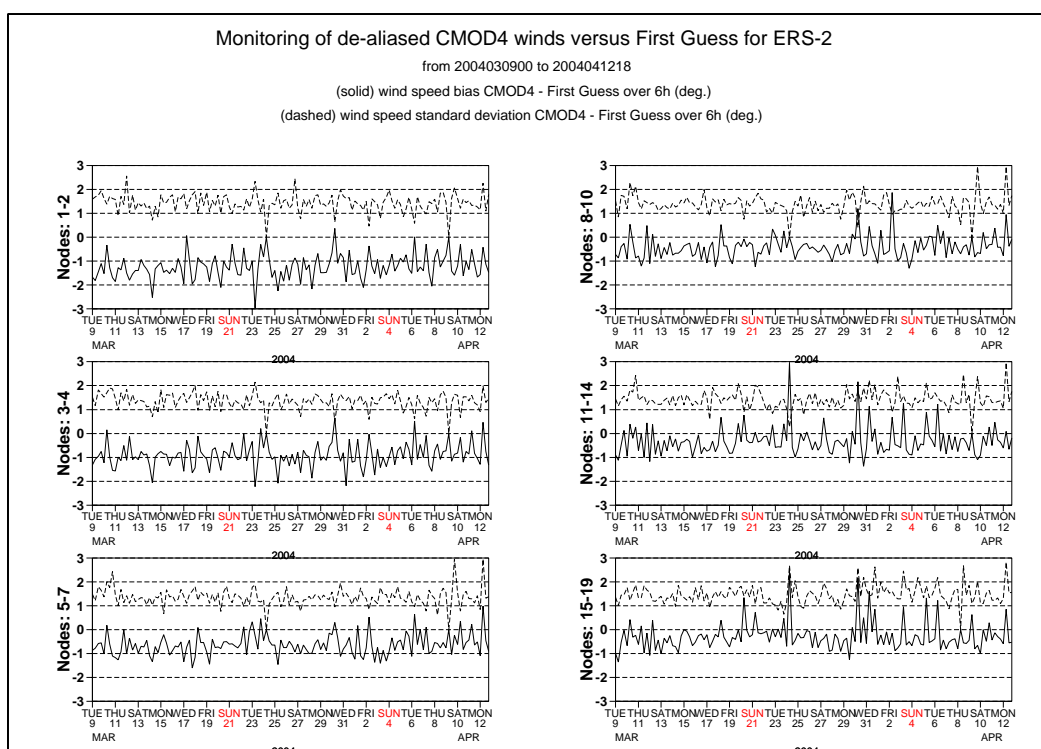


**FIGURE 14.** Same as Fig.13, but for the de-aliased CMOD-4 wind. Statistics are computed only for wind speeds higher than 4 m/s.Cycle 93

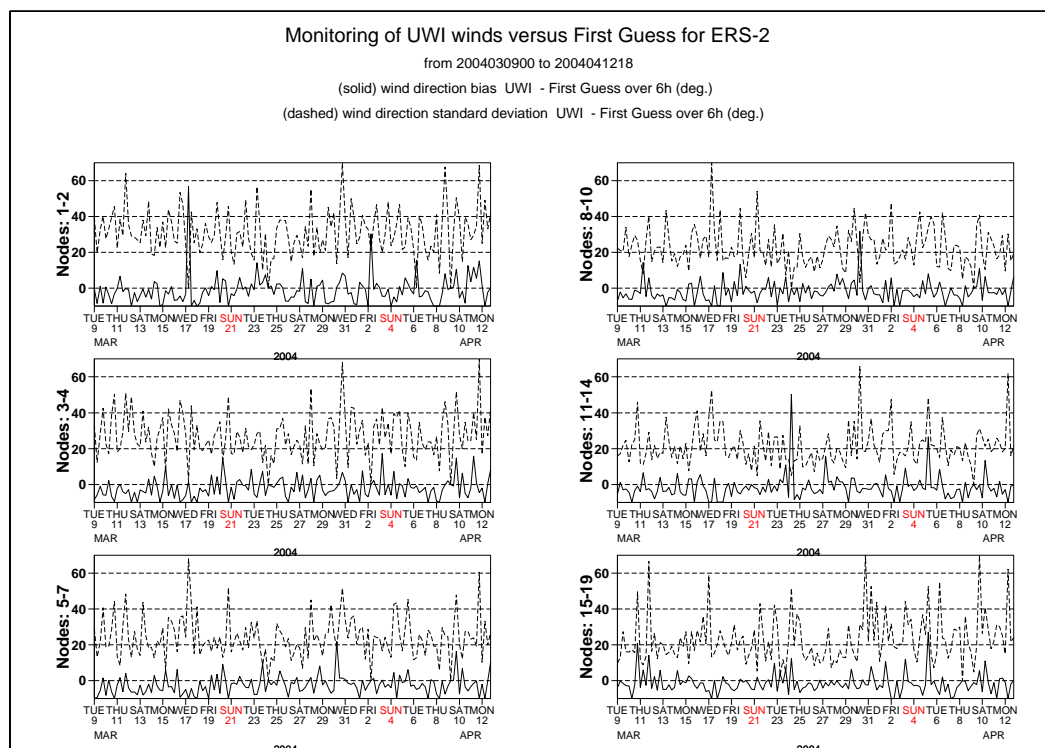


FIGURE 15. Same as Fig. 13 but for wind direction.Cycle 93.

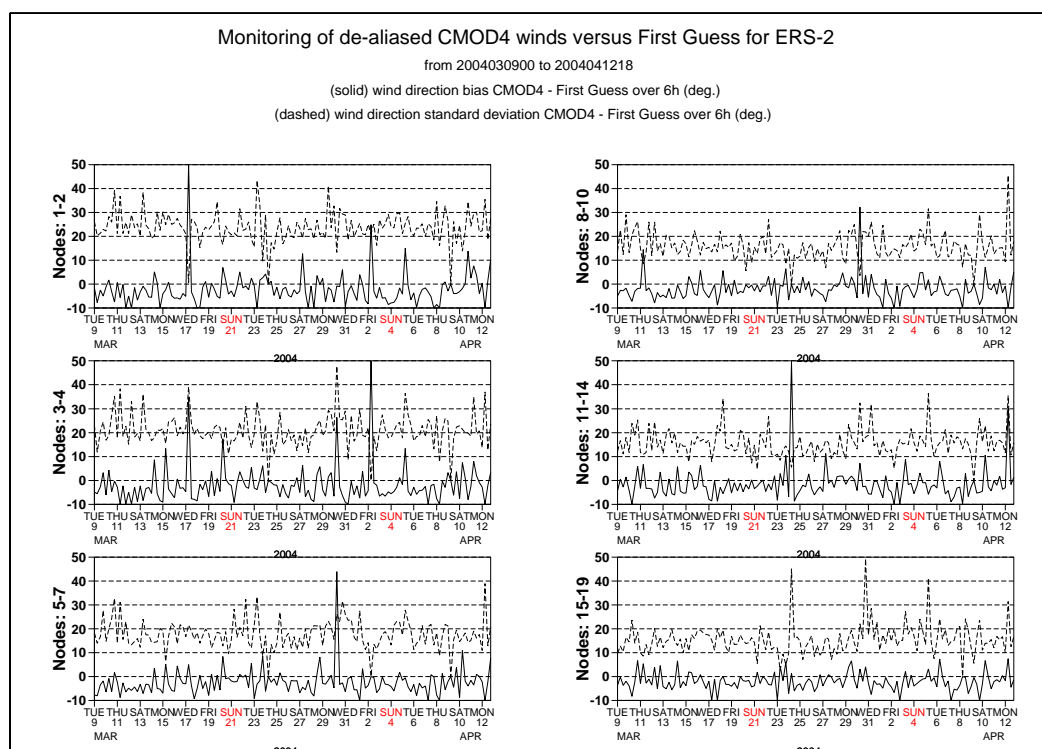
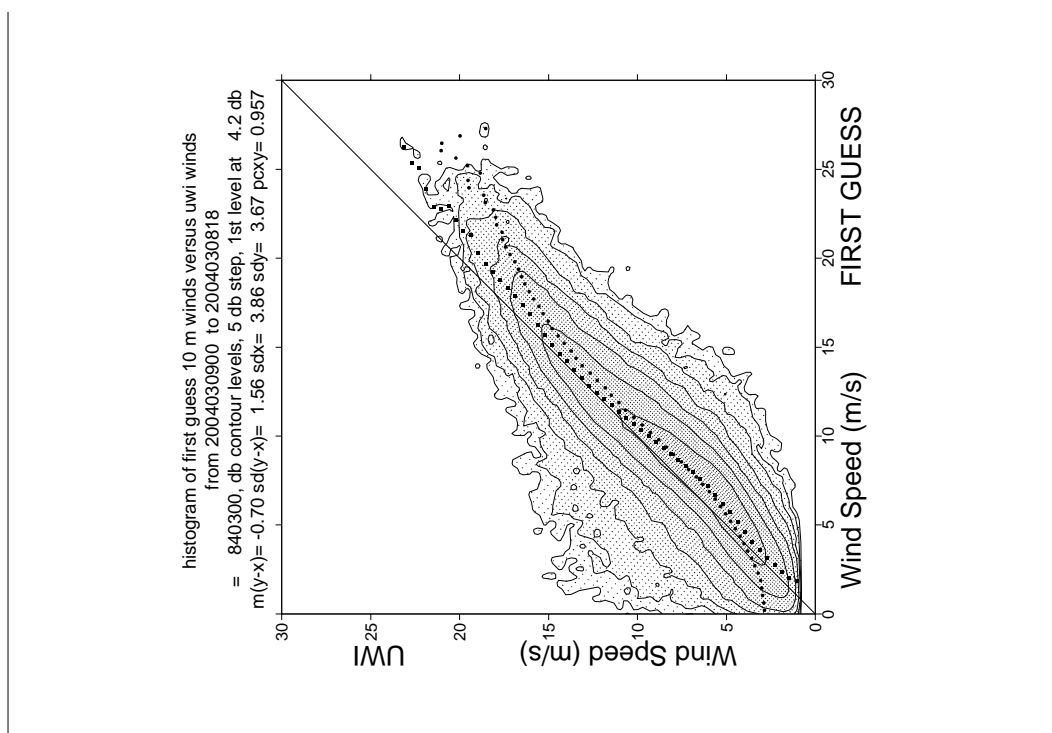
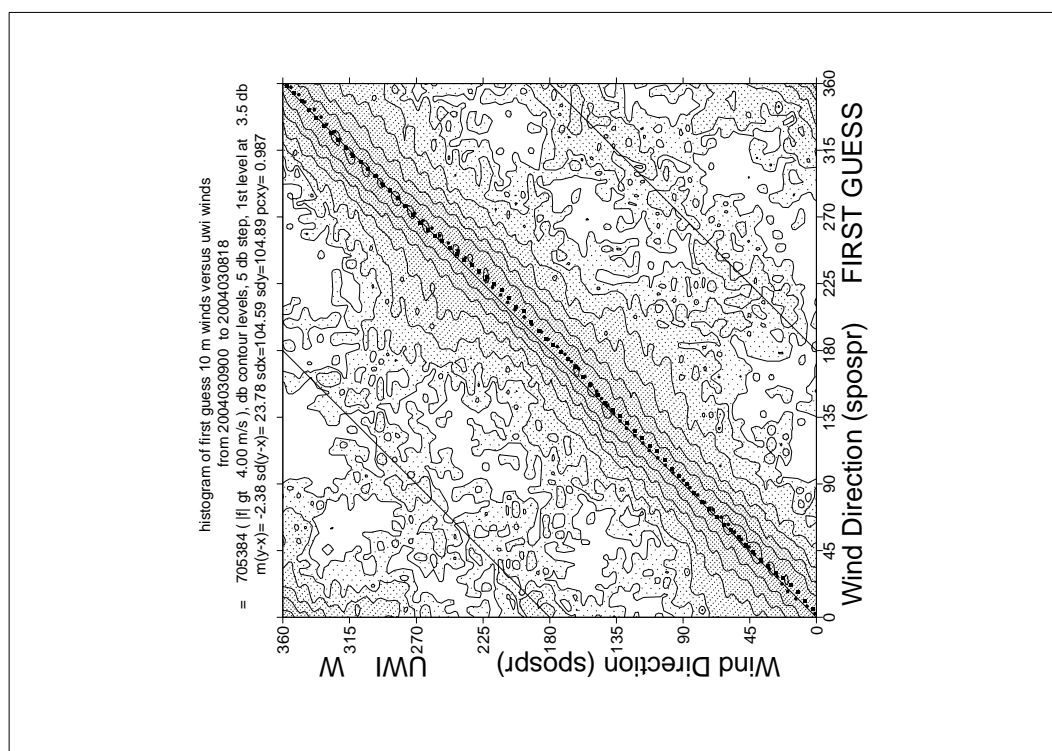


FIGURE 16. Same as Fig. 14 but for wind direction. Cycle 93.





**FIGURE 17.** Two-dimensional histogram of first guess and UWI wind speeds, for the data kept by the quality control. Circles denote the mean values in the y-direction, and squares those in the x-direction. Cycle 93



**FIGURE 18.** Same as Fig. 17, but for wind direction. Only wind speeds higher than 4m/s are taken into account. Cycle 93.



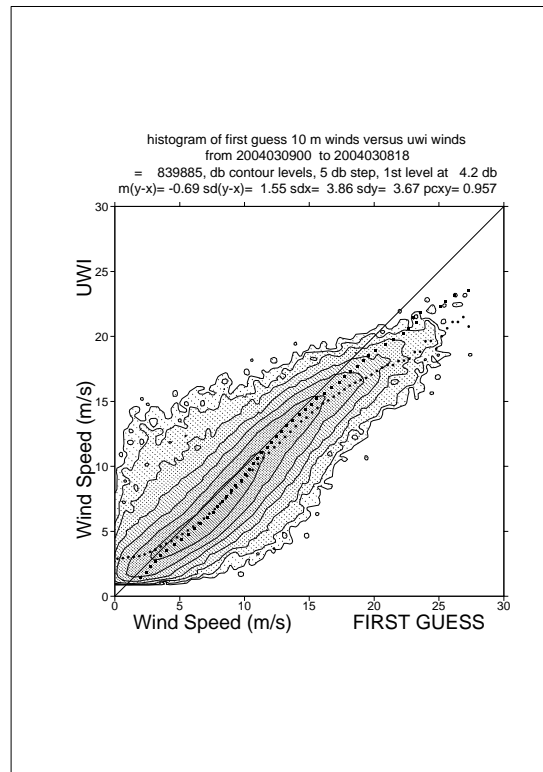


FIGURE 19. Same as Figure 17 but for de-aliased CMOD-4 winds. Cycle 93

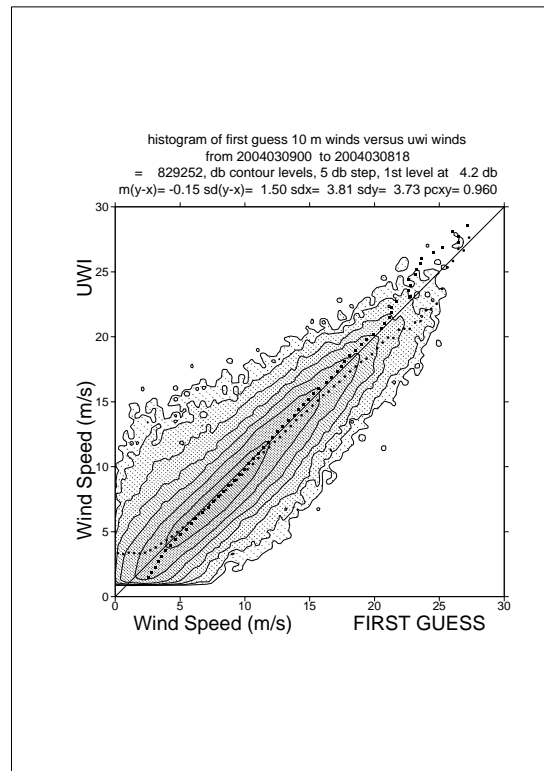


FIGURE 20. Same as Figure 17 but for de-aliased CMOD-5 winds. Cycle 93

## **5.0 Yaw error angle estimation**

The yaw error angle estimation is computed on-ground by the ESACA processors. The full set of results of the yaw processing is stored in an internal ESA product named HEY (Helpful ESA Yaw) disseminated from the ground station to ESRIN. The estimation of the yaw error angle is based on the Doppler shift measured on the received echo. That estimation can be done with a good accuracy only for small yaw error angle (in the range between  $\pm 4$  deg.). Above that range, due to high Doppler frequency shift the signal spectrum is outside the receiver bandwidth and the yaw estimation is strongly degraded. Details regarding the yaw processing can be found on the following document (chapter 9): <http://earth.esa.int/pcs/ers/scatt/articles/soamain-030521.pdf>

The yaw error angle estimation aims to compute the correct acquisition geometry for the three Scatterometer antenna throughout the entire orbit. The Yaw error angle information is used in the radar equation to derive the calibrated backscattering (sigma nought) from the Earth surface and to select the echo samples associated to one node. In ESACA the definition of the node position is as the one adopted in the old processor (for details see: [http://earth.esa.int/pcs/ers/scatt/articles/scatt\\_work98\\_processing.pdf](http://earth.esa.int/pcs/ers/scatt/articles/scatt_work98_processing.pdf)). In such way the distance between the nodes (both along and across track) is kept constant (25 Km) and what is changing in function of the yaw error angle is the number of echo samples that contributes to the node calculation and the incidence angle of the measurement. This is why the three scatterometer antennae could see the node with a different geometry due to an arbitrary variation of the yaw angle along track. The number of samples that actually contributes to a node and the yaw flag can be retrieved from the UWI Data Set Record (DSR) product. For that reason the definition of few fields in the UWI product has been updated. For details see the Scatterometer cyclic report - cycle 90 -.

The Figure 21 (since beginning of HEY dissemination) and Figure 22 (cycle) show for each orbit the average doppler frequency shift (first 3 plots Fore Mid and Aft antenna), the minimum, maximum and mean yaw (fourth plot), the yaw standard deviation (fifth plot) and the percentage of source packets acquired with a yaw error angle outside the range  $\pm 2$  degrees (sixth plot).

The result of the yaw monitoring for cycle 93 is a yaw error angle within the expected nominal range ( $\pm 2$  degrees) with an average level around 0 deg. for most of the orbit. On 23 and 28 March 2004 some orbits had a bad quality yaw performances due to the satellite manoeuvres occurred on those days.

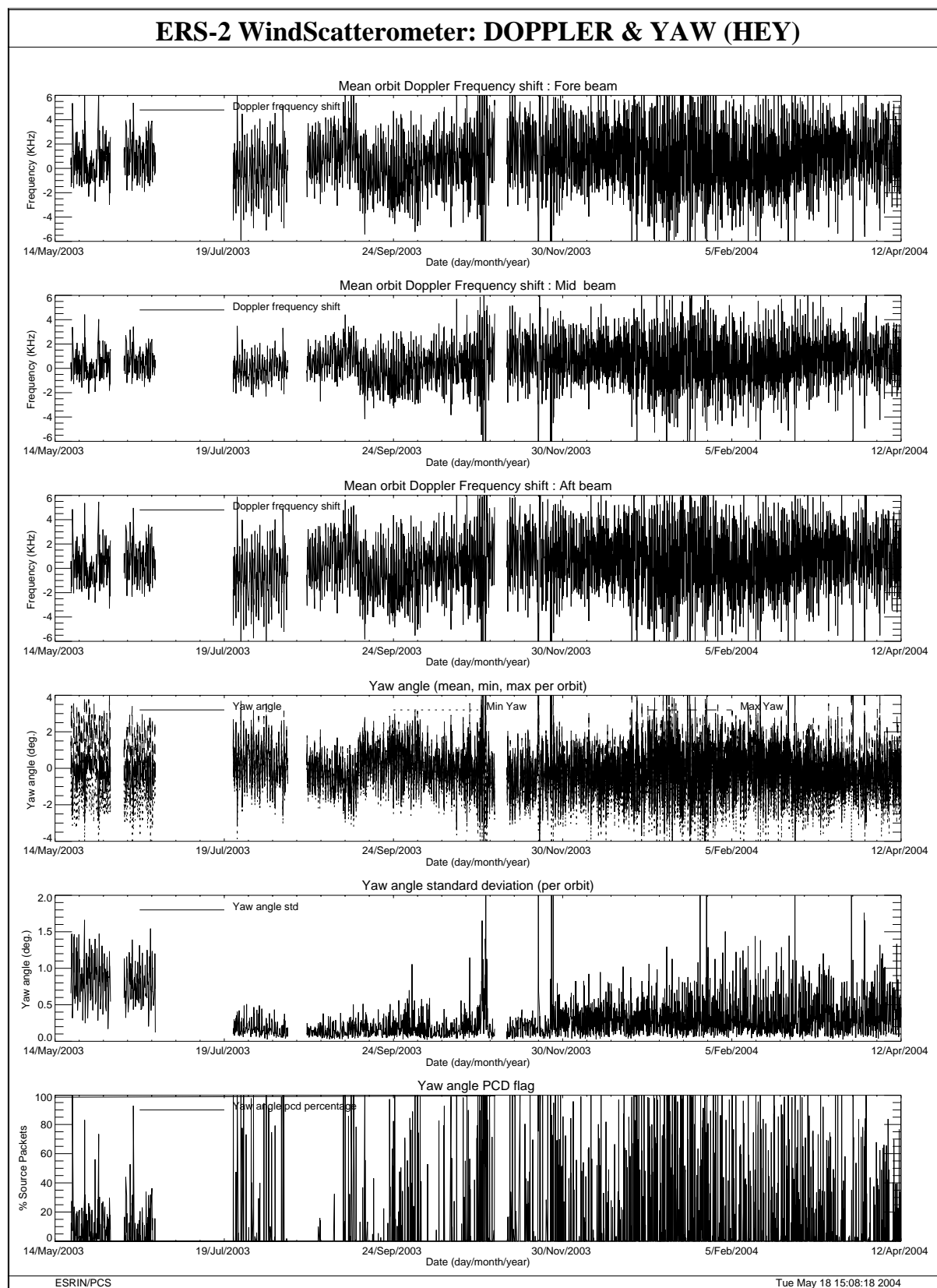


**FIGURE 21. Doppler frequency shift and Yaw angle monitoring since the beginning of HEY data dissemination (15th May 2003).**

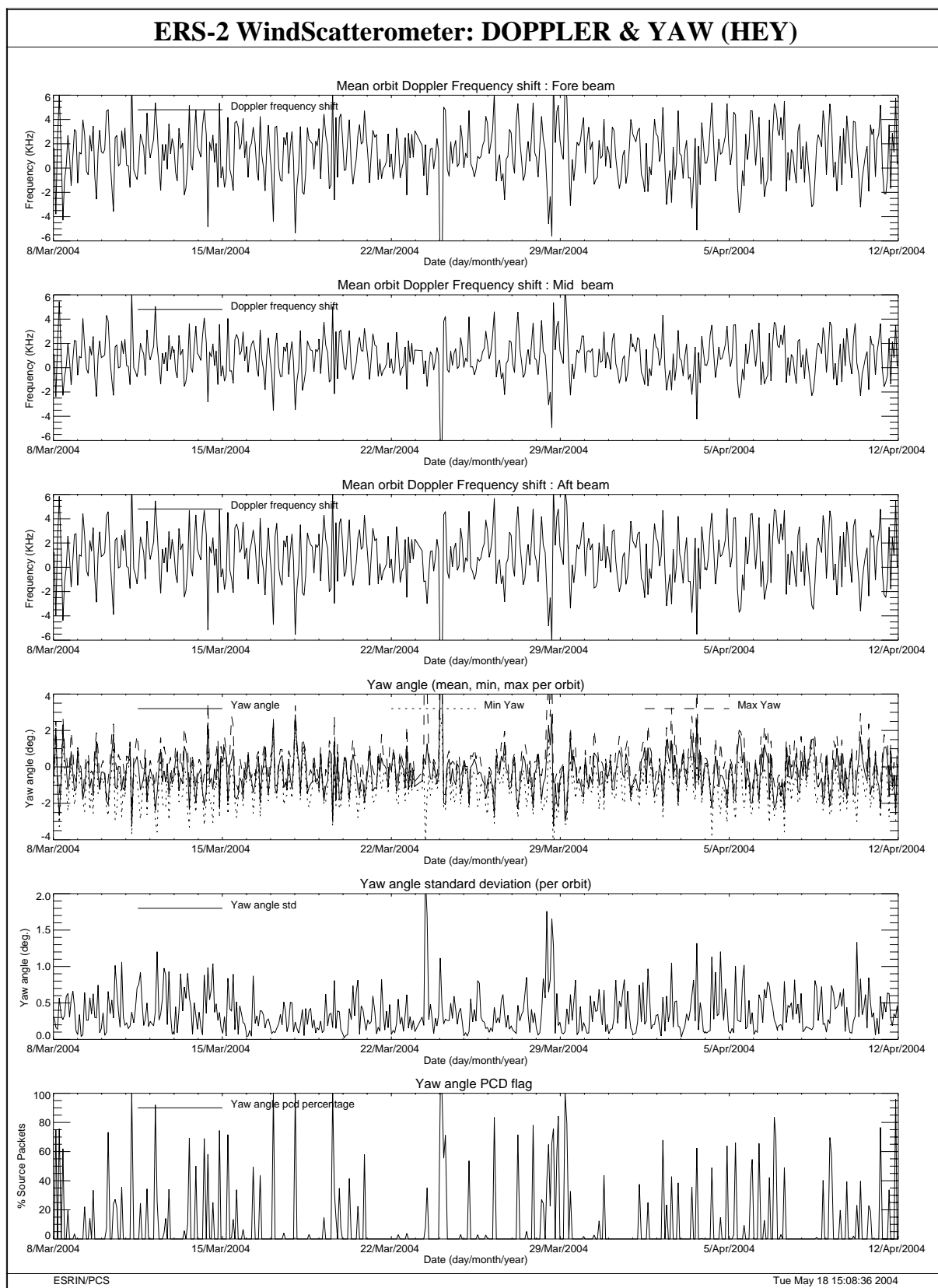


FIGURE 22. Doppler frequency shift and Yaw angle monitoring for cycle 93.

